END

DATE
FILMED

4-82

DTIC

1.0

4.5
5.0

2.8

2.5

3.2

2.2

3.6

2.0

1.1

4.0

1.8

1.25

1.4

1.6

MICROCOPY RESOLUTION TEST CHART

NATIONAL BUREAU OF STANDARDS 1963 A

AD A112472

OFFICE OF NAVAL RESEARCH

Contract N00014-81-K-0516

TECHNICAL REPORT NO. 1

Time-Dependent Morphologies and

Viscoelastic Properties of Block Copolymers

by

Jeffrey C. Kelterborn and D.S. Soong

Prepared for Publication

in the

Polymer Engineering and Science

University of California, Berkeley
Department of Chemical Engineering
Berkeley, Ca. 94720

March 16, 1982

82 03 24 022

REPORT DOCUMENTATION PAGE		READ INSTRUCTIONS BEFORE COMPLETING FORM
1. REPORT NUMBER Technical Report No. 1	2. GOVT ACCESSION NO. AD-A/12 472	3. RECIPIENT'S CATALOG NUMBER
4. TITLE (and Subtitle) Time-Dependent Morphologies and Viscoelastic Properties of Block Copolymers		5. TYPE OF REPORT & PERIOD COVERED Technical Report May 1, 1981 - present
		6. PERFORMING ORG. REPORT NUMBER
7. AUTHOR(s) Jeffrey C. Kelterborn and David S. Soong		8. CONTRACT OR GRANT NUMBER(s) N00014-81-K-0516
9. PERFORMING ORGANIZATION NAME AND ADDRESS Department of Chemical Engineering University of California at Berkeley Berkeley, Ca. 94720		10. PROGRAM ELEMENT, PROJECT, TASK AREA & WORK UNIT NUMBERS
11. CONTROLLING OFFICE NAME AND ADDRESS Office of Naval Research Arlington, VA 22217		12. REPORT DATE March 15, 1982
		13. NUMBER OF PAGES
14. MONITORING AGENCY NAME & ADDRESS(if different from Controlling Office)		15. SECURITY CLASS. (of this report) Unclassified
		15a. DECLASSIFICATION/DOWNGRADING SCHEDULE

16. DISTRIBUTION STATEMENT (of this Report)

This document has been approved for public release and sale; its distribution is unlimited

17. DISTRIBUTION STATEMENT (of the abstract entered in Block 20, if different from Report)

18. SUPPLEMENTARY NOTES

19. KEY WORDS (Continue on reverse side if necessary and identify by block number)

Morphology, Time-Dependent Properties, Block Copolymer, Dynamic Mechanical Properties.

20. ABSTRACT (Continue on reverse side if necessary and identify by block number)

Dynamic mechanical properties of block copolymers over a wide temperature range have been previously correlated with the phase-separated microstructure of these systems. In the present work the morphology of the block copolymer is altered by large tensile deformation at various temperatures. Upon removal of the applied stress the morphological features of such stretched-and-released systems become functions of time, as the non-equilibrium microstructure reverts to a thermodynamically stable state. This reformation

DD $_{1 \text{ JAN } 73}^{\text{FORM}}$ 1473   EDITION OF 1 NOV 65 IS OBSOLETE

S/N 0102-LF-014-6601

process is monitored by dynamic mechanical measurements with a modified torsion pendulum capable of applying both tensile and torsional deformation. Experimental results are analyzed using a modified Nielsen model to obtain information on the time-dependent structural state of the samples. These results are then compared with stress-strain curves to provide further insight into the structure breakdown-reformation mechanisms. Two competing mechanisms, domain fracture and block pull out, are proposed to explain these experimental observations.

Accession For

NTIS CRA&I	☑
DTIC T S	☐
Unannounced	☐
Justification	

By

Distribution/

Availability Codes

Avail and/or

Dist Special

A

DTIC
COPY
INSPECTED
2

INTRODUCTION

Superior engineering properties can often be achieved through the mixing of different polymers. For example, rubbers are added to plastics to impart a high impact strength, while plastics are used to stiffen rubbers. Commercial block copolymers commonly consist of rigid and rubbery components. In SBS, the styrene-butadiene-styrene triblock co-polymer used in this study, the central elastomeric poly-butadiene block is bonded on both ends to rigid polystyrene blocks. This arrangement leads to a unique combination of desirable physical properties, making these copolymers commercially important (1).

The degree of mixing and state of aggregation in such mixed polymer systems is dictated by the Gibbs free energy of mixing. The very small entropy gain of mixing macromolecules and the usually positive enthalpy of mixing result in a net positive free energy, and hence immiscibility and phase separation (1,2). However, in block copolymers, the size of the component blocks and the presence of chemical linkages between blocks limit the phase separation to a microscopic scale, often referred to as microphase separation (1).

The existence of multiple phases gives rise to distinct glass transitions. For SBS, this is evidenced by two maxima

in the viscous damping curves ($G''(T)$)(3). In contrast, a single intermediate transition would be expected of a single-phase system of mixed composition. Optical transparency is another indication of phase separation in the samples. A single-phase system is optically clear, whereas multiphase systems can range from transparent to opaque depending on the size of the individual phases. Macrophase separation in physical blends of the same constituents results in sample opacity. However, microphase separation of block copolymers usually gives slightly hazy but nearly transparent samples, as the domain size is too small to scatter much visible light(2).

The tensile properties of block copolymers also reflect their heterogeneous nature(1). Stress-strain curves of the first loading cycle often exhibit an initial rapid rise in stress, followed by a yielding and drawing region. This is typical of plastic behavior. However, the high extensibility to ultimate failure is characteristic of a rubber. In the unloading cycle there is substantial strain recovery. Thus the plastic-like specimen becomes rubber-like at the completion of the first loading cycle. The second cycle is now rubber-like and does not show any yielding and necking phenomena. After the strain has been removed, the specimen undergoes a slow but spontaneous healing process and eventually regains its original plastic-like behavior.

The stress-softening phenomenon observed in the initial loading cycle is termed the strain-induced plastic-to-rubber transition (4). This, along with the subsequent "healing" process, has been the focus of considerable

research efforts. Various methods have been used to follow the structure breakdown and reformation. These include electron microscopy, small-angle X-ray scattering, surface hardness and tensile behavior. As will be discussed later, conclusive evidence concerning the rate and mechanism of structure breakdown and reformation has yet been firmly established.

In this work the structure reformation is monitored by measuring the storage and loss moduli as functions of time following a large deformation and release of strain. Analysis of these results is based on extending the classical structure-property relationships to a time-dependent level. This permits a microscopic interpretation of both the structure breakdown and reformation processes, and offers new insights into the results of previous research. The time-dependent dynamic mechanical measurements are then coupled with tensile testing to determine the effective morphological states dictating local and long-range deformations. Before these results are presented, we will first review some of the relevant concepts associated with the morphologies and viscoelastic properties of block copolymers.

PREVIOUS WORK

The microphase separation in block copolymers can re-
sult in various morphologies. Five ideal domain structures
are postulated, depending on the polymer composition (5).
For a composition extreme in one direction, a large amount of
the major component forms a continuous matrix with spherical
inclusions of the minor component. As the fraction of the
minor component is increased, the inclusions change from
spheres to cylinders. Near equal proportions, alternating
lamellar structure prevails where both phases are continuous.
However, the co-continuous phase-separated structure may not
be physically perfect, i.e., there may exist local breaks or
discontinuities in the phases. Nevertheless, sufficient
long-range order remains so that the system mechanical pro-
perties behave as if phase continuity were maintained. This
is analogous to the case of a fiber-reinforced composite
wherein long fibrous fillers (also discontinuous) achieve a
strengthening effect independent of their L/D ratio when L/D
is very large, when the material is stressed parallel to the
fiber orientation (6). As the once-minor component starts to
predominate, a phase inversion occurs whereby the formerly
major component now forms cylindrical and finally spherical
domains.

Several models have been developed which predict the
morphology of block copolymers using statistical thermody-
namics approaches. Perhaps the earliest model was developed
by Meier (7,8) for AB copolymers. Leary and Williams (9,10)

later recognized that an interphase must exist with finite thickness. They were able to predict successfully the favored morphology for triblock copolymers. Helfand (11) used a mean field approach to predict domain size as a function of molecular weight. His predictions agree well with experimental results. Inoue and coworkers (12) and Soen and coworkers (13) considered solvent casting of triblock polymer films and postulated that as the solvent evaporates from a polymer solution a critical micelle concentration is reached at which the domains are formed.

The viscoelastic properties of block copolymers strongly depend on the state of microphase separation. In the solid state, the storage (G') and loss (G") moduli over a broad temperature range reveal considerable information about elastic and viscous parameters associated with not only the individual domains but also the interphase (14-16). Two major transitions are generally observed corresponding to the glass temperatures of the two homogeneous polystyrene-rich and polybutadiene-rich phases. The magnitudes of peaks in G"(T) have been shown proportional to the relative amounts of those phases (17). Diamant and coworkers (14-16) showed that the viscoelastic behavior between the two transitions is dictated by the interphase. They developed a model to fit the G' and G" data over a broad temperature range, and correlated the height and the shape of the plateau region in G" with the amount of interphase and the composition profile across it.

The existence of phase separation also dictates much of the melt behavior of SBS. Holden and coworkers (18) presented viscosity versus temperature data for an ABA block copolymer and its pure components. At low temperatures the block copolymer viscosity lies between those of its constituents. However, at higher temperatures the viscosity of the block copolymer becomes greater than that of both constituents. This synergistic behavior was attributed to a phase separation between the two components that resists mixing by the applied shear.

Several models have been developed to predict moduli of heterogeneous systems from the properties of the constituent phases. These may be roughly divided into two categories. The first calculates moduli from an idealized picture of the actual structure. The second entails calculations based on an equivalent assembly of mechanical elements with properties identical to those of the individual constituents. These elements are connected either in series or in parallel.

Kerner (19) developed expressions for the static shear and bulk moduli of a composite composed of soft spherical

dispersoids embedded in a hard matrix. Christensen (20) extrapolated these equations to predict complex viscoelastic moduli. Both give satisfactory agreement with experimental data. However, neither adequately represents the inverse case of hard dispersoids in a soft matrix (1). Dickie (21) was able to extend the Kerner equation to account for a partial phase inversion.

Takayanagi (22) also examined the soft dispersoids-hard matrix composite but based calculations on an equivalent mechanical model. This model represented the actual composite by a mixture of series and parallel coupling of the pure components. The degree of mixing and composition of the composite was reflected in the fraction of series and parallel coupling.

Halpin and Tsai (23,24) proposed a more general equation that covers both morphologies - soft dispersoids in a hard matrix and hard dispersoids in a soft matrix. Nielsen (6) modified the equations to accommodate the complete range of morphology, invoking the concept of the maximum packing fraction of the dispersoids and the co-continuity of the phases.

The present work focuses on the dynamic mechanical behavior of block copolymers with the goal of establishing

time-dependent structure-property relationships. The polymers are of a composition such that both phases are partially continuous. In view of this, Nielsen's model was adopted as the basis for data analysis.

The nonlinear stress-strain behavior of a block copolymer also depends on its morphology and the tensile behavior of its constituents. Holden and coworkers (18) studied the stress-strain behavior of SBS with various polystyrene contents. They found that the magnitude of the stress at a given strain level depended on composition, increasing with the volume fraction of the rigid phase. At low polystyrene content the material behaved in a rubber-like fashion while at high polystyrene content plastic-like behavior was observed. Above 53% polystyrene a yield point was observed at low strains, characteristic of a plastic. However, as the strain was further increased a drawing region was observed followed by a high xtension to failure, characteristic of a rubber. When the stress was removed the sample showed a set ("permanent" deformation) that slowly decreased with time. If the sample was loaded again, rather than allowed to recover over a long time, considerable hysteresis was observed, and the material behaved like a rubber over the entire (second) loading cycle. Holden and coworkers suggested that this hysteresis, or stress softening, may possibly be due to a breakdown of a stress-supporting polystyrene structure.

Considerable research efforts have been devoted
to the study of the effects of morphology on the mecha-
nical behavior of a block copolymer. These commonly
involve changing the morphology of a given system
and examining the subsequent changes in mechanical
properties. There are several ways in which the mor-
phology can be changed. One method is to cast the polymer
from different solvents. Selective solvation of one block
causes those chains to expand in solution, but leaves the
chains from the other block in a collapsed state. This pro-
motes the continuity of the block that is preferentially dis-
solved while casting (evaporating the solvent), even though
it may be a minor component of the copolymer. Aggarwal and
coworkers (25) present stress-strain curves of Kraton 1101
(28% PS) cast from tetrahydrofuran/methyl-ethylketone
(THF/MEK), carbon tetrachloride (CT) and benzene/heptane
(BH). These solvents have solubility parameters of approxi-
mately 9.2, 8.6 and 8.3, respectively. Only the THF/MEK-
cast specimen exhibits a plastic-like yielding and draw re-
gion in the first loading cycle. The other two specimens do
not exhibit this yielding phenomenon, but behave like filled,

crosslinked rubber. These investigators suggested that the THF/MEK preferentially dissolves the polystyrene block, enhancing its continuity and thus causing the plastic-like yielding. This conclusion follows from the fact that the solubility parameter of polystyrene, 9.1, is closest to that of THF/MEK. The continuity of polystyrene was confirmed by electron microscopy. Beecher and coworkers (26) noted that the initial slope of the CT curve is somewhat greater than that of the BH curve, suggesting slightly more continuity among the polystyrene domains. The solubility parameter of CT is closer to that of polystyrene than is BH, confirming their hypothesis. Kalfoglou (27) compared three SBS specimens cast from MEK, cyclohexane (good solvents for polystyrene and polybutadiene, respectively) and toluene, a common solvent for both components. The magnitude of first loading curves and yield stresses were in the same order as the "goodness" of the solvents for polystyrene, with the highest curve resulting from the MEK-cast specimen. Pedemonte and coworkers (28) altered the morphology of extruded SBS samples by pre-swelling in n-heptane, a good solvent for polybutadiene, then drying the samples to constant weight. As the pre-swelling time was increased the height of the yield peak decreased and the entire curve shifted downward until, for two hours of swelling, the stress-softening effect disappeared. They attributed these results to a disruption of the polystyrene domain continuity by the swollen polybutadiene. This was confirmed by electron micrographs of the swollen structure. Akovali and coworkers (30) blended SBS

with homopolymers of polystyrene to enlarge the styrene do-
mains. They found that the SBS-PS blends had a higher ini-
tial yielding and first loading curve than the pure SBS,
consistent with their hypothesis of the enlargement of
polystyrene domains leading to greater continuity.

Chen and Cohen (30) examined the influence of block
molecular weight on the tensile behavior of an ABA block co-
polymer. They blended two copolymers in various ratios to
vary the number-average molecular weight of the blocks in a
systematic fashion while maintaining the polystyrene content
in the range of 25-28%. They found that molecular weight
changes at constant composition exerted a strong influence
on the stress-softening effect and the rate-dependence of
the stress-strain behavior. Increasing the polystyrene
block molecular weight from 7,000 to 16,000 caused a signifi-
cant rise in the first-cycle stress-strain curve and a pro-
nounced decrease in the sensitivity of the stress-strain be-
havior to strain rate. The interphase fraction was assumed
to decrease with increasing block number-average molecular
weight (i.e., domain dimensions increased but interphase
thickness remained relatively constant). Since the polysty-
rene content was held relatively constant, the authors con-
cluded that the interphase fraction dictated much of the
observed tensile behavior.

Processing techniques have been shown to have a signifi-
cant effect on morphology and therefore the engineering
properties of a block copolymer. Beecher and coworkers (26)

compared the stress-strain curves for Kraton 101 (28% PS) cast from THF/MEK and prepared by compression molding. The yield point observed in the first elongation of the solution-cast specimen was absent in the compression molded sample. However, the second loading cycle for both samples was identical. Pedemonte and coworkers (31) present micrographs of extruded Kraton 1101 specimens (28% PS) that show the cylindrical polystyrene domains are oriented parallel to the extrusion direction. This morphology can be made still more ordered by annealing, achieving a long range, "single crystal" structure (32,33). Compression molded samples of the same polymer also show cylindrical domains, but they are arranged in a more random fashion and do not form an effectively continuous polystyrene phase. This accounts for the absence of the stress-softening effect in compression molded samples of Beecher and coworkers (26).

The stress-strain behavior of these "single crystal" specimens show considerable anisotropy. Keller and coworkers (32,33) showed that stretching the extruded plugs parallel to the extrusion direction reveals plastic-like behavior, whereas perpendicular deformation reveals rubber-like behavior. Leblanc (34) also observed anisotropic behavior in star-shaped butadiene styrene block copolymer samples prepared by extrusion and injection molding. Samples displayed rubber-like behavior when stretched perpendicular to the molding flow direction and plastic-like behavior parallel to the flow direction.

Pedemonte (31) searched for possible effects of solvent evaporation rate on toluene cast films of Kraton 1101. Changing the evaporation rate from 0.5 cm^3/hr to 20 cm^3/hr had no noticeable effect on morphology or stress-strain behavior.

Thus far we have summarized some of the most important developments to date, including the various thermodynamic, viscoelastic and equivalent mechanical models, the linear and nonlinear properties exhibited by these block copolymers, and the effects of processing variables on the morphology and engineering properties. These basic factors promoted the present work which studies the rates and mechanisms of structure variation occurring in a block copolymer subjected to a large deformation. The time-dependent morphologies and viscoelastic properties of block copolymers have been an area of considerable research. Our work has undoubtedly benefited from these previous efforts. We will now go on to briefly summarize the current understanding and remaining questions, and see how this work sheds new light on this subject.

BLOCK COPOLYMERS UNDERGOING STRUCTURAL CHANGES

The tensile behavior of certain block copolymers displays a prominent stress-softening effect whereby repeated straining to the same extension results in lower stresses. Research in this and related areas has been summarized in the reviews by Dawkins [35], Estes and coworkers [36] and Aggarwal [37].

Hashimoto and coworkers [4] termed the stress-softening effect of the first loading cycle the strain-induced plastic-to-rubber-transition. They noted that at the yield point in the first loading cycle a sharply defined neck appears which, upon further elongation, gradually encompasses the entire sample. Their micrographs of microstructure in the necked region showed that at 85% elongation there is shearing, kinking and orientation of the polystyrene domains ("chevron" patterns are formed). Further stretching produced a more extensive fragmentation. However, this structure breakdown is reversible. Micrographs of a sample released from 600% elongation and rested for several days at room temperature showed considerable reformation of the original morphology.

Reformation was shown to be accelerated at higher temperatures. Micrographs of a sample released from 600% elongation and annealed at 100°C for two hours showed nearly total reformation of the original structure. This also indicates that the structure breakdown during the first loading cycle is followed by a spontaneous reformation process.

Previous researchers have measured various polymer properties in order to follow the morphological changes during the structure breakdown-reformation process. Beecher and coworkers (26) used Kraton 101 (28% PS) and compared the stress-strain response of the reforming structure to that of the original material. They found the "healing" process slow at room temperature -- after 41 days the height of the "first-cycle" yield peak was still 25% lower than the original yield peak. However, heating the specimen at 93°C (still lower than the polystyrene glass transition) totally reformed the original stress-strain response in 8 minutes.

Canter (38) examined structure reformation while stress-relaxing SBS specimens (Thermolastic 125, 25% PS) at high elongation. Specimens were stretched to 150% and held for five days at room temperature. After releasing, the torsional modulus was determined after 10 seconds around the polystyrene transition ($\approx 100^{\circ}$C). Comparison with the unstretched sample revealed a sharpening of the modulus

transition. Canter concluded that prestretching led to a more uniform ordering of the polystyrene domains.

Akovali and coworkers (29) compared viscoelastic properties of Kraton 1101 before and after stretching through the plastic-to-rubber transition. Immediately after stretching, significant changes were observed in the plateau region, whereby the tan δ(T) curve was elevated, the E'(T) curve was lowered while the E"(T) curve remained unchanged. Annealing this sample at 110°C for 2 hours returned the curves to their positions before stretching except for the appearance of a small peak in tan δ and E" around -40°C. Niinomi and coworkers (39) continued this study with micrographs of samples before and after stretching. A micrograph of SBS (blended with polystyrene) taken after stretching showed parallel striations across the polystyrene regions and more lighter areas within the structure. They speculated that these striations may be crazes induced by stretching. The small peak in tan δ and E" observed near -40°C by Akovali and coworkers (29) may correspond to an increase in the "mixed region", similar to the explanation of the small peak in the damping curve of CCl_4-cast SBS seen by Beecher and coworkers (26). They observed that an increase in the mixed region could account for the lighter areas seen in the micrographs after stretching.

Leblanc (34) noted that star-shaped butadiene styrene block copolymers stretched to 100%, released, and held at 60°C showed a progressive recovery of the original stress-

strain behavior -- at a temperature significantly lower than the glass temperature of the rigid polystyrene. He hypothesized that the material in the interphase and not the polystyrene is responsible for the stress-strain behavior, including the stress-softening effect and subsequent structure reformation. Leblanc used a thermomechanical analysis technique to examine samples before and after stretching. This technique records the displacement of a surface contact probe as a function of temperature. Distinct transitions between room temperature and $90^{\circ}C$ disappeared after stretching. The polystyrene glass transition near $100^{\circ}C$ was absent from all curves, even those of samples before stretching. Leblanc suggested that the disappearance of transitions between room temperature and $90^{\circ}C$ may correspond to the destruction of the interphase upon stretching. Further experiments were done measuring the surface hardness of a stretched and released sample at temperatures from $40^{\circ}C$ to $60^{\circ}C$. Immediately after stretching and releasing, the surface hardness dropped and then gradually returned towards its original value before stretching. Leblanc was able to fit the hardness recovery kinetics with a linear dependence on the logarithm of time, except for the hardness immediately after stretching and releasing, i.e., at the y-intercept, t=0. At $40^{\circ}C$, the logarithmic law predicted a lower hardness than was actually measured at short times while at $60^{\circ}C$ the logarithmic law overpredicted the measured data. The origin of these deviations was unclear. Leblanc concluded that the

idea of a rigid structure breakdown during the first elongation is incompatible with hardness recovery at temperatures lower than the glass temperature of the rigid phase. Hence the yielding and stress softening was attributable to the breakup of the interphase.

In addition to the micrographs discussed earlier, Hashimoto and coworkers (4) examined changes in the equatorial SAXS intensity distribution around the first-order maximum during structure reformation at room temperature and at 60°C. The sharp distribution peak of the original SBS sample (48.2% PS) totally disappeared upon stretching to 500%. At room temperature no significant recovery of the original distribution was seen up to 4 hours while complete recovery was achieved in 10 minutes at 60°C. After 10 minutes the peak became more intense than the original, suggesting an increased regularity of the domains -- an annealing effect. This work was supplemented by comparisons of the complex tensile moduli of unstretched specimens and specimens held at 330% elongation determined over a broad temperature range. The authors attributed a shift of the polybutadiene dispersion from -80°C to -100°C upon stretching to a decrease in free volume, while the shift of the polystyrene dispersion from 90°C to 80°C was attributed to fragmentation of the polystyrene domains. In the stretched state a rapid decrease in E' was noted around 40°C which, the authors concluded, arose from a large increase in the amount of interface due to the fragmentation of the polystyrene

domains.

Yang and Meinecke (40) studied the stress-softening effect in block copolymers of 15-30% polystyrene by measuring the tensile stress and the energy dissipation simultaneously as a function of strain. This was done by stretching the sample to a certain strain, measuring the stress, then superimposing a small-amplitude sinusoidal strain to measure the energy loss per cycle for a unit volume of material. This was done for strains through the stress-softening effect up to $\varepsilon=1.8$. Data were presented as plots of stress versus strain and energy loss versus strain. The energy loss exhibited a marked peak at the same strain where the yield point occurred. When a second run was repeated after resting the sample at room temperature for 24 hours the loss peak had reformed but the original stress-strain behavior did not. Structure reformation was followed by measuring the energy loss as a function of time on a previously stretched sample held at the strain where the energy loss peak was initially observed. Similar to the hardness recovery measured by Leblanc (34), the energy loss data were linear with the logarithm of time. The peak in the energy loss versus strain curve was followed by a plateau region. The authors speculated that this peak corresponds to an initial structure breakdown after which no further structural changes occur, hence the plateau in the energy loss curve. They hypothesized that the structure is broken into stable, isolated, polystyrene filler particles for which the Guth-

Gold-Einstein equation (41) for the stress-strain properties of filled systems applies. This was found to be the case except for the 30% polystyrene sample. Electron micrographs of this sample elongated to $\epsilon=1.8$ confirmed that the polystyrene lamellae did not break into individual particles as did the cylindrical domains of the other samples.

Kaelble and coworkers (42) analyzed the stress-strain behavior and optical properties of SBS at various temperatures with the idea of reversible, interfacial debonding and subsequent void formation between domains (which may or may not involve breakage of covalent bonds at the block junctions). In their mathematical model, the observed tensile stress is a product of two functions, one accounting for the rigid behavior of the styrene phase and the other accounting for the rubber elasticity of the butadiene phase. The first loading cycle displayed a smooth transition between these two functions, the former describing the linear portion prior to yielding, the latter describing the behavior at high elongation. They combined the two functions into a general stress-strain relation involving $B(t,\epsilon)$. This function is determined by strain, time (during stretching and releasing) and temperature and varies between zero and one. Kaelble and coworkers studied the tensile behavior of SBS with various loading and unloading cycles and backed out a single universal curve of $B(t,\epsilon)/B_o$ versus tensile strain, where B_o is the initial value before stretching. They concluded that the function B is capable of correlating the tensile behavior with interfacial debonding and bonding. In addition, they discovered that λ_m, the model parameter des-

cribing the physical crosslinking of the styrene phase, was constant for stress-strain cycles at temperatures up to $40^{\circ}C$. This indicated the stability of the fragmented styrene domains as physical crosslinks, in agreement with the conclusions of Yang and Meinecke (40). However, for stress-strain cycles at temperatures greater than $40^{\circ}C$ λ_m steadily increased. The authors suggested that this may correspond to polystyrene chain segments being pulled out of their domains.

The loss of sample transparency observed at high elongation (where B approaches zero) and the regain of transparency when the sample was released (B approaches 1) were used as evidence to support the concept of reversible interface debonding. This cavitation process was quantitatively analyzed by using a spectrophotometer to study the optical transmission properties. Structure reformation was followed through the change in sample absorbance, from maximum absorbance for a highly elongated sample to greatest transparency for the undeformed sample. Micrographs of a sample held stretched for 16 hours showed agglomerated cavities and cracks formed by coalescence and growth of primary cavities. Released, the specimen showed simple planes of defects which, the authors concluded, were the collapsed cavities and surface cracks. Kaelble and Cirlin (43) applied the Halpin-Polley model (44) for kinetics of micro defect growth to develop a physical interpretation of the B function. Cavitation was found to proceed in two steps -- an initial nucleation stage followed by a propagation and cavity coalescence stage at higher elongations. They showed that the work loss due to cavitation could be correlated directly with the work of interfacial adhesion between the styrene and butadiene phases.

Having examined what is currently known of the mechanical behavior of block copolymers, particularly tensile and dynamic mechanical properties, we are now in a position to discuss our work and show how it adds a new understanding to some aspects of the time-dependent morphology and properties of block copolymers. After outlining our experimental procedure, results of this work will be presented and discussed in detail in the balance of this paper.

EXPERIMENTAL SECTION

The SBS samples used in this study were provided by the Shell Development Company. These are designated as TR-41-1648 and TR-41-1649. Table 1 lists some important sample specifications and structural information.

Each polymer was dissolved in a mixed solvent of tetrahydrofuran (THF)/methylethylketone (MEK) (at a 90 to 10 volume ratio) to a concentration of about 9% by weight. These solutions were filtered to remove solid contaminants.

Samples were prepared by spincasting from the solutions In this process the solvent was allowed to evaporate overnight in a hood, leaving a polymer film on the inside of the drum. This procedure was repeated until the desired sample thickness was reached.

The polymer was dried at $60^{\circ}C$ under vacuum until it reached a constant weight and then annealed at $110^{\circ}C$ for one hour. The entire drying process usually required approximately 2 weeks.

Specimens for tensile testing were cut with an X-acto knife and a "dog-bone" shaped metal template. Typical sample dimensions were 20mm x 5mm x 2.5mm. The critical curvature at the four corners of the dog-bone samples was cut with a sharpened, hollow metal tube used in a drill press.

Rectangular specimens for the torsion pendulum were cut with a circular knife turned in a milling machine at 1160 rpm. Typical dimensions were 50mm x 15mm x 4mm. Water was used as a cooling fluid in this cutting process.

The mechanical properties of these materials were

measured with an Instron tensile testing machine and a modified torsion pendulum. The Instron was a standard table type, model TM-S, manufactured by the Instron Corporation The torsion pendulum, a free-oscillation device, has been extensively described in the literature. The particular instrument used in this study was constructed in-house and modified to permit elongation of the samples. Figure 1 gives a schematic diagram of the main components of this instrument. It consists of a sample

holding system, a torsion bar to apply an oscillating torque to the sample, and a recording system that measures the rate at which the angular oscillation damps out. The sample holding system was designed to allow elongation to large strains followed by rapid return to a stress-free state. A detailed drawing of the clamps is shown in Figure 2. Both clamps are equipped with a spring-loaded wedge assembly. As shown in Figure 1 the lower clamp can be raised and lowered by a screw-motor system so that the specimen can be stretched and relaxed. The spring-loaded wedges firmly grip the specimen during the stretching as well as the unloading cycle.

The specimen and clamps are contained in a Statham Temperature Test Chamber (model SD70) capable of controlling temperature to within $\pm 0.5^{\circ}C$ in the operating range of $-180^{\circ}C$ to $200^{\circ}C$. Above-ambient temperatures are achieved with the chamber functioning as a convection oven while subambient temperatures are maintained by flowing liquid nitrogen through a solenoid control valve. A window is mounted in the front panel, allowing visual examination of the specimen during testing at ambient and above-ambient temperatures.

The top clamp is freely suspended by a stiff, steel wire

to minimize extraneous damping caused by the instrument. The weight of the upper clamp and its attachments is counter-balanced by a counterweight assembly to ensure that the specimen is in a stress-free condition during testing.

Movable weights are attached to the torsion bar to adjust its inertia, thus setting the oscillation at the desired frequency. The amplitudes of successive oscillations of the torsion bar are recorded by the cross-polarizer system described below.

A six-volt lamp shines through two polarizer filters to a photomultiplier tube. One of these filters is attached to the torsion bar, while the other is firmly affixed to the window of the photomultiplier tube. Angular displacement of the top clamp from its equilibrium position causes the attached filter to deviate from the cross-polarized config-uration, allowing light to pass through the filter attached to the photomultiplier tube. The oscillation of the torsion bar is thus transformed into oscillating electrical signals generated by the photomultiplier. This output is then re-corded on a strip-chart recorder and the damping characteris-tics of the polymer are analyzed.

Tensile behavior of the SBS samples was studied using the standard Instron procedure at a nominal strain rate $(\dot{\ell}/\ell_o)$ of 50%/min. to 300% elongation. All runs were done at room temperature. The cross-sectional area of the samples was measured with a micrometer to within ± 0.005mm. This was used to convert output of the load cell (f) into stress, $\sigma = f/A$.

In studying the time-dependent properties of SBS with the torsion pendulum, a sample is first stretched to 300% elongation and released to the stress-free state immediately before testing. Upon completion of the stretch and release process, the dynamic mechanical properties of the sample are determined as a function of time at the controlled temperature. In addition to the changing damping characteristics, sample length contracts and the width and thickness expand. The viscoelastic properties measured with the torsion pendulum are very sensitive to the sample dimensions, particularly the thickness, necessitating accurate measurement of these time-dependent dimensions. This was achieved by using two specimens of identical length, width and thickness. The first is used to determine the dimensions as a function of time after stretch and release. The second allowed measurement of the damping characteristics as a function of time following stretch and release at the same temperature. The storage (G') and loss (G") moduli are then calculated based on the time-dependent dimensions. This procedure is discussed in detail below.

The original dimensions of the sample were measured with a micrometer as mentioned previously. The length of the specimen in-between the clamps was measured with a cathetometer, which determines the distance between the two pins shown in Figure 3. To this was added the distance from the end of the pin to the point where the sample "begins," i.e., the last point of contact with the wedge in the clamp.

Since the sample is enclosed in the temperature chamber during a run, a special procedure, other than using a micrometer, had to be developed to monitor the variation of the sample dimensions. Through the window in the front panel the length is monitored by following the distance between the pins mounted to the wedges in the clamps. Figure 3 illustrates how the thickness and width were measured. A mark is first enscribed across the width and thickness of the sample. The image of the thickness mark was reflected by a fixed mirror. The length of the width mark on the sample as well as the reflected thickness image were measured with a custom-made, horizontal cathetometer. Since the direction along the sample width and the reflected image may not be perfectly parallel with the axis of micrometer traverse, a constant correction factor must be developed to accommodate angles of the mirror, cathetometer, etc. This was determined by comparing the sample width and thickness as seen by using the cathetometer with those actually measured with the micrometer.

Prior to stretch and release, the sample was heated to the desired temperature and the counterweight assembly was adjusted to offset the mass of the top clamp, torsion rod and other attachments to the top clamp. Small, solid blocks were then fitted between the torsion bar and the temperature chamber to immobilize the top clamp. The bottom clamp was lowered and the sample elongated to 300%. The deformed sample was quickly returned to the point at which the torsion

bar just lifted away from the constraining blocks. At this
point, the sample was in a stress-free state. Subsequent
dimension recovery was thus unimpeded as no residual tensile
stress persisted in the sample.

In measuring the time-dependent dynamic mechanical proper-
ties, the sample was again preheated to the test temperature
and kept at this condition for 30-40 minutes. The polarizing
filter on the top clamp was adjusted so that minimum light
was transmitted to the photomultiplier tube when the torsion
bar was at its equilibrium position. The strip-chart re-
corder was then zeroed.

Just before testing, the sample was stretched to 300%
and returned to the stress-free condition in the same manner
as described previously. This process lasted 40-50 seconds
depending on the polymer and specimen size. Dynamic mechani-
cal data were then taken by nudging the torsion bar and
measuring the resulting frequency and successive maxima of
the oscillation from the damped sinusoid on the strip-chart
recorder. The weights were moved along the torsion bar to
ensure the desired frequency. The time-dependent moduli and
complete temperature scans were measured at 1.0 ($\pm$.05) Hz and
0.5 ($\pm$.05) Hz, respectively. It required 3-4 minutes to
position the weights properly so that these frequencies were
achieved. This procedure was repeated periodically for the
remainder of the run.

The damping data were first analyzed to determine tan δ

which in turn was used with the time-dependent dimensions to calculate G' and G". The calculation procedure first derived by Nielsen (45,46) was used for data analysis.

While the complete temperature scan of the moduli is being done, the sample is in its original unstretched condition so that the dimensions stay constant. Subambient temperatures are achieved by flowing nitrogen vapor in thermal equilibrium with liquid nitrogen through a solenoid control valve. At these low temperatures an "anti-fogging" disc must be used. This is a plastic disc that is attached around the top clamp just under the torsion bar. It prevents the fog leaving the chamber from contacting the polarizing filters and interfering with the recording of the torsion bar motion.

RESULTS AND DISCUSSION

Stress-Strain Behavior

The phenomena of strain-induced plastic-to-rubber tran-
sition and subsequent structure reformation are first ex-
amined through analysis of stress-strain properties. Re-
sults for TR-41-1649 are shown in Figure 4. The first load-
ing cycle exhibits an initial rapid rise of stress followed
by a drawing region beyond the yield point. At this point,
a neck forms which, upon further stretching through the
drawing region, propagates along the length of the samples.
Upon completion of neck propagation the stress again rises
until the sample ultimately ruptures at large strain, nearly
1000%. This high extensibility is characteristic of a rub-
ber. However, the initial high modulus and the observed
yielding phenomenon are both characteristic of a plastic.
This plastic-like behavior may be caused by the connectivity
of the polystyrene phase in the samples. Upon yielding, a
substantial fraction of this originally continuous polysty-
rene phase is disrupted, and the sample resembles a filled
rubber with the rigid polystyrene domains acting as fillers.

The transparency of the necked region during the first
loading cycle is noticeably less than the rest of the
sample. This loss of optical clarity suggests the creation
of internal voids and light scattering surfaces whose aver-
age size exceeds the wavelength of visible light. This
observation is consistent with the work of Kaelble and

coworkers (42) in which optical properties of block copoly-
mers undergoing tensile deformation were studied.

In the unloading of the first cycle, the sample re-
trieves most of its original dimensions, thus accomplishing
substantial strain recovery. This is again characteristic of
a rubber. The second loading cycle from the unloaded condi-
tion immediately following the first loading cycle is indica-
tive of rubber-like behavior, and does not show any yielding
phenomenon. The deformation of the first cycle has apparent-
ly caused a structure transformation that changed the sample
from a plastic-like to rubber-like state.

If the sample is allowed to rest in a stress-free con-
dition for three hours between the first and second cycles a
partial structure reformation is observed (Figure 4). Here
a small, rapid rise in stress is initially observed, indicat-
ing that the polystyrene phase has partially reformed its
original connectivity.

Reformation is accelerated at higher temperatures.
Figure 4 shows the stress-strain curves for two samples that
have been annealed at $110^{\circ}C$ for two hours. One sample (solid
line) was annealed continuously for two hours after it was
spin cast and dried. The other sample was annealed for one
hour, stretched to 300% and released (destroying the struc-
ture) and immediately annealed for another hour (reforming
the structure). After cooling to room temperature the
sample was stretched to 300%, producing the loading curve
shown by the dashed line in Figure 4. Destruction of

structure by a large deformation and subsequent reformation via annealing resulted in a slight increase in stress. This may be a consequence of a more pronounced, long-range ordering, promoted by the alignment of the rigid phase by the applied large deformation. However, this result and its interpretation are both inconclusive as experimental errors in sample cutting and dimension measurement produce an uncertainty in the stress-strain curves of approximately 10% (not shown in the figure) which obscures the difference in the two curves. Previous workers have reported complete return of the original stress-strain properties after annealing (36).

Several theories (4,26-31,34,39,40,42,43) have been developed to explain the tensile behavior of block copolymers, particularly the stress-softening effect accompanying the first loading cycle. Most have attributed this effect to either breakdown of the interphase or to breakdown of a stress-supporting polystyrene network. This difference is further complicated in that the interphase may be considered either a diffuse region of mixed composition between the two major phases or simply a sharp boundry between phases. Tensile deformation may destroy the (diffuse) interphase and/or fragment the rigid phase, creating more surface area and hence more (sharp) interface. In this section, interphase

destruction is considered a possible cause of the stress-softening effect while creation of more interface by the disruption of the rigid phase will be discussed later.

Chen and Cohen (30) suggested that the tensile behavior of block copolymers depends on the amount of interphase. As mentioned earlier, this conclusion was based on the significantly different stress-strain behavior of specimens with similar polystyrene contents but varying block molecular weights, and hence varying fractions of interphase (7,8) In addition, SBS specimens swollen in isooctane and re-dried showed a significant lowering of the stress-strain curve and a decrease in stress-to-failure. The authors attributed this to a disruption of the interfacial region by the swelling process.

Leblanc (34) used a thermomechanical analysis (TMA) technique which records the displacement of a surface contact probe as a function of temperature. In SBS samples, distinct transitions observed below the glass transition of polystyrene were associated with the interphase. These transitions disappeared upon stretching and releasing the specimens which suggested interphase alteration upon deformation. Hence, it was concluded that interphase disruption dictates the first-cycle tensile behavior.

Most theories propose that stress-softening is attributable to the breakdown of a stress-supporting polystyrene network (4,26-29,31,39). This is confirmed by electron micrographs of specimens at high deformation which show the breakup of polystyrene domains. However, the state of the interphase cannot be detected in these micrographs. The swelling experiments of Pedemonte and coworkers (28) indicated that loss of polystyrene connectivity leads to the stress-softening effect.

Theories on the stress-softening effect and the subsequent structure reformation in SBS have assumed opposing viewpoints on the importance of the interphase and the polystyrene phase. Experimental evidence, including stress-strain properties and electron microscopy, have been provided to support both viewpoints. However, very little work has been pursued with dynamic mechanical testing. This technique provides substantial information about the domains and the interphase (14-16). In this work, dynamic mechanical testing is used to advance our understanding of the role of the interphase and polystyrene phase in the stress-softening effect and its associated structure breakdown-reformation processes.

Dynamic Mechanical Properties of Reforming Structures

Dynamic mechanical measurements of block copolymers are commonly made over a broad temperature range encompassing the glass transitions of both blocks. When this method is applied to the study of structure breakdown and reformation, the time-dependent morphology complicates the situation. At

low temperatures ($T \ll T_g^{PS}$) the morphology variation is relatively slow, but at temperatures above ambient, particularly approaching T_g^{PS} ($\approx 100^\circ C$) the morphology rapidly changes so that a complete temperature scan of a deformed sample never corresponds to any given (static) morphology. This problem is not unique to dynamic mechanical spectroscopy but occurs with any broad temperature scan of a reforming structure, e.g., Leblanc's TMA curves (34). Because of this inability to scan the complete G', G" spectra without substantial morphological change during testing, this study was a new approach...time-dependent dynamic mechanical measurements. Experiments are done under isothermal conditions and G', G" determined as functions of time at a given frequency.

Dynamic mechanical properties of samples listed in Table 1 following stretch (to 300%) and release are presented in Figures 5 to 10. Note that a run at a particular temperature involves stretching the specimen at that same temperature.

The G' data in Figures 5 and 8 show that structure breakdown and reformation is much more significant in TR-41-1649 (1649) than in TR-41-1648 (1648). This was expected since the stress-softening effect in the stress-strain curve is much less pronounced for 1648 (4). Increasing the temperature from $35^\circ C$ to $60^\circ C$ has a negligible effect on the

initial value and drop-off in 1648 as measured by G' (Figure
8), but results in a slightly greater reformation speed as
expected from an activated process. Results for 1649 (G'
plot of Figure 5) show a greater drop-off at 35°C from the
initial value, yet this G' curve recovers faster than that
at 60°C. After five hours, G' at 35°C returns closer to its
initial value than the corresponding behavior at 60°C. Con-
sidering reformation to be an activated process, this is a
surprising observation and will be fully discussed later.

The G" data in Figures 6 and 9 show only a small change in the
values measured during reformation from the initial G" before stretch
and release. Note G" is derived from measured tan δ and G',
and thus is very sensitive to accumulated experimental errors
in these quantities, resulting in the observed data scatter.
However, the data can be fitted to a straight line, the in-
tercept of which reveals considerable information about the
temperature effects on structure breakdown. The simplicity
of this analysis warrants a brief discussion using G" data.
Temperature effects on the G' data will be interpreted at
length later.

The intercept is, in principle, a measure of G" imme-
diately after release of the sample (t=0). The decrease
from the original G" (before stretching) to this intercept
(immediately after stretch and release) indicates the degree
to which the structure governing G" (e.g., the interphase

structure) at the given temperature is broken down. For 1649 (Figure 6) the decrease is 16% at 35°C and 26% at 60°C, and for 1648 (Figure 9) 15% at 35°C and 22% at 60°C. At the higher temperature the structure is broken down, or perhaps more specifically, the interphase is altered to a greater extent than at the lower temperature, suggesting that following elongation at different temperatures the reformation process begins with different morphologies.

It is known that G" is sensitive to the amount of interphase and the composition profile across it, while G' is relatively independent of the interphase (14-16). Our results show a significant change in G' and a small change in G" upon the initial stretching and structure breakdown, suggesting that breakdown does not involve the interphase to a great extent. The small change in G" throughout our experiments also suggests that the interphase is not strongly involved in recovery, either. A breakdown and reformation of a large-scale, stress-supporting network may be involved. In addition, the rate of change of G' and G" as revealed by the time-dependent dynamic mechanical measurements is generally much slower than the time scale of experimentation, i.e., the rate at which each measurement is taken. Hence, during the measurement of each datum point (about 10 sec.), the morphology of the system can be treated as essentially static. The reverse problem of the viscoelastic measurement affecting the inherent structural reformation process is also nonexistent, as the applied perturbation is very

small and the occurrence is only intermittent. The information obtained via dynamic mechanical spectroscopy can therefore be used to infer structural details of block copolymers exhibiting unaffected morphology variation as a function of time. This non-interfering technique can be applied to the same system at different temperatures to study the effect of this parameter on the structure breakdown and reformation processes.

Upon completion of the four experimental runs, samples were annealed in nitrogen at 110°C for one hour (Figures 5 to 10). This resulted in approximate return to the initial values before elongation and suggests possible reformation of the original structures. Deviations from the exact initial values, particularly in G", may be attributed to experimental errors. As mentioned earlier, G" is derived from tan δ and G' and is proportional to the cube of the sample thickness. Thus it is extremely sensitive to accumulated experimental errors in these quantities. Several G" must be determined to average out the experimental errors. Moreover, measuring G' and G" at only two temperatures limits the structure examination to very local situations. An examination of the global situation, encompassing a wide temperature range, is necessary to determine conclusively if structure reformation leads to recovery of the original domain environment.

To determine the structural state of the samples after annealing we performed temperature scans from -120°C to

$100^{\circ}C$ with the torsion pendulum. The magnitude of the polystyrene and polybutadiene glass transition peaks in the G"(T) curves has traditionally been associated with the relative amounts of styrene and butadiene in their respective domains (35). Recently, Diamant and coworkers (14-16) have shown that the plateau between the two transitions is extremely sensitive to the amount of interphase region and the composition profile across it.

In this experiment we compared two new samples. The first was annealed in nitrogen at $110^{\circ}C$ for two hours while the second was annealed for one hour, cooled to room temperature, stretched to 300%, released and annealed for another hour. Both samples have been annealed for two hours so that the "annealing effect" (4), i.e., greater structure uniformity from longer annealing, is eliminated. Figures 11 to 13 show that the temperature scans of tan δ, G' and G" for both specimens are identical. Hence, we can conclude that reformation proceeds back to the original structure with the same amount of material in the domains and interphase and with the identical composition profile within the interphase. This rather remarkable behavior will be explained below.

The schematic drawing in Figure 14 summarizes the behavior of the dynamic mechanical properties (for TR-41-1648 and TR-41-1649) throughout the low-temperature ($T<110^{\circ}C$) reformation process. At long times, the recovery is extremely slow. It may require infinite time for the structure to

reform totally. However, our complete temperature scans of the viscoelastic properties show that annealing in nitrogen at $110^{\circ}C$ returns the properties, and hence the structures, back to their initial values. Just after stretching and releasing (structure breakdown) tan δ increases, G' drops and G" slightly decreases. This is in agreement with the results of Akovali and coworkers (29) who performed complete temperature scans on Kraton 1101 samples and found that just after stretching and releasing (in the plateau region) tan $\delta(T)$ was elevated, E'(T) was lowered while E"(T) remained unchanged. However, contrary to our findings, after annealing the stretched-and-released-samples in nitrogen at $110^{\circ}C$ a small peak near $-40^{\circ}C$ appeared in tan $\delta(T)$ and G"(T) which was not seen in the unstretched samples. They postulated that the existence of this peak could be attributed to a large increase in the interphase caused by stretching that persisted even after annealing. This discrepancy from our findings is not fully understood at present. However, Diamant and coworkers (14-16) showed that a maximum in G"(T) between the two main transitions could be attributed to a "bulge" in the interphase composition profile.

The application of dynamic mechanical testing has proven effective in studying structure breakdown and reformation. It is particularly useful since the intermittent, small perturbation does not interfere appreciably with structure recovery but still provides substantial structural information. In addition, the morphology at the end of the

reformation process can be determined by a complete temperature scan. The procedure to infer the morphology immediately after structure breakdown and during the reformation process from the time-dependent dynamic mechanical properties will be described below.

Morphology During Elongation and After Release of Strain

The application of composite theories to the fragmented structures of samples at high deformation has not been extensively explored. Previous work on SBS showed that under high deformation the fragmented polystyrene domains behave as independent filler particles in a polybutadiene matrix (40,42,43). However, the structure immediately after the sample is released and during reformation has not been examined. This will be done using composite theories to infer structural changes from the time-dependent material properties measured during structure reformation. A modified Nielsen model, discussed below, is used to analyze time-dependent G' of the reforming structure.

The Nielsen model (6) is used to predict the modulus of a heterogeneous material from the morphology and pure component properties. It employs, as limiting cases, the Halpin-Tsai equations (23,24) which determine the composite moduli when one phase is dispersed in the other continuous matrix. However, the Nielsen model accommodates the morphology at systems in all composition ranges, and in

particular, systems with co-continuous phases. For a morph-
ology of hard dispersoids in a soft, continuous phase (the
"Regular System" by Nielsen's convention) the modulus is
given by:

$$M = M_1 \; \frac{1 + AB\phi_2}{1 - B\psi\phi_2}$$ (1)

where: and:

M_1 = modulus of the continuous phase $B = \dfrac{M_2/M_1 - 1}{M_2/M_1 + A}$

M_2 = modulus of the dispersed phase

ϕ_{max} = maximum packing fraction of $\psi = 1 + \dfrac{1 - \phi_{max}}{(\phi_{max})^2}\,\phi_2$
       the dispersed phase

                                $A = k - 1$

ϕ_2 = volume fraction of dispersoids

k = Einstein coefficient
$\left(= \dfrac{7 - 5\nu}{8 - 10\nu} \text{ for spherical dispersoids} \right)$

ν = Poisson's ratio

As shown in Figure 15 the predicted modulus increases with
the fraction of dispersed rigid phase, but it fits experi-
mental data only at low volume fractions of the rigid phase.
For the opposite morphology of soft dispersoids in a hard,
continuous phase (Nielsen's "Inverted System") the composite
modulus is given by:

$$M = M_1 \frac{1 - B_1 \psi \phi_2}{1 + A_i B_i \phi_2} \qquad (2)$$

where:

M_1 = modulus of the continuous phase

M_2 = modulus of the dispersed phase

ϕ'_{max} = maximum packing fraction of the dispersed phase in the inverted system

ϕ_2 = volume fraction of dispersoids

and:

$$B_1 = \frac{M_1/M_2 - 1}{M_1/M_2 + A_i}$$

$$\psi = 1 + \frac{1 - \phi'_{max}}{(\phi'_{max})^2} \phi_2$$

$= (\frac{1}{A}$ when the morphology of the dispersoids is identical to those in the "Regular System," an uncommon situation.)

This equation applies to high amounts of the rigid phase, and the predicted modulus of this system decreases with increasing fractions of the soft dispersoids (Figure 15). Equations 1 and 2 give different predictions between $1 - \phi'_{max}$ and ϕ_{max} which form the upper and lower bounds of experimentally determined values. This is because in this region the dispersed phase in either case is no longer truly dispersed, and both phases may, in fact, be co-continuous. Nielsen proposed that the upper and lower bounds (for inverted and regular systems) be averaged logarithmically:

$$\log M = \phi_U \log M_U + \phi_L \log M_L \ , \qquad\qquad (3)$$

$$\text{or } M = M_U^{\phi_U} \cdot M_L^{\phi_L}$$

where ϕ_U is the fraction of rigid material that is effectively continuous and ϕ_L is the fraction of soft material that is effectively continuous. These parameters, ϕ_U and ϕ_L, thus denote the degree to which the material is represented by the idealized one-phase continuous morphology. For a polystyrene composition, ϕ_{PS}, between $1-\phi'_{max}$ and ϕ_{max} (Figure 15) :

$$\phi_U = \frac{\phi_{PS} - (1-\phi'_{max})}{\phi_{max} - (1-\phi'_{max})} \quad (4) \quad \text{and} \quad \phi_L = \frac{\phi_{max} - \phi_{PS}}{\phi_{max} - (1-\phi'_{max})} \quad (5)$$

Upon release of a sample from high strain, the polystyrene domains, initially fragmented and behaving as filler particles, now conglomerate to reform their original domains. This structural reformation hypothesis can be tested using the Nielsen model to calculate G' for polystyrene dispersoids in a continuous polybutadiene matrix and comparing it with the first experimental G' measured after releasing the sample from high deformation.

If the originally co-continuous polystyrene phase is broken down by the applied large strain so that it is no longer continuous, then the modulus of the system (immediately after stretch and release) is given by that for polystyrene dispersoids in a polybutadiene matrix, i.e., Equation 1 for Nielsen's "Regular System." This equation applies to any system morphology with an elastomeric matrix phase and a

dispersed rigid phase (6). However, to use this equation it is necessary to know the morphology of the system to determine reasonable values for the adjustable parameters. In particular, the arrangement of the rigid, dispersed phase must be known. This may seem an intractable problem since the morphological state of the degraded structure is an unknown to be determined. However, reasonable assumptions can be made concerning the morphology just after stretch and release to facilitate computation of its modulus.

As mentioned earlier, Yang and Meinecke (40) found that upon high deformation, lamellar domains in SBS samples broke into cylinders. From the micrographs of Hashimoto and co-workers (4) it can be seen that TR-41-1649 samples prepared in the same manner as in this study do exhibit a lamellar morphology. Therefore, we can be reasonably certain that just after stretch and release the TR-41-1649 samples have cylindrical polystyrene dispersoids. However, micrographs of TR-41-1648 show that the polystyrene does not have a lamellar morphology, but there are still connections among the domains forming a "swirl-like" structure (4). We assumed that upon high deformation this structure is also broken down into dispersed cylinders. It might be argued that these cylinders could be broken down still further into spheres. However, by assuming cylindrical dispersoids for both TR-41-1648 and TR-41-1649 at high deformation we in fact overestimate the modulus of the system just after stretch and release, and this is our desired direction to use

as clarified below. Since, in Equation 1, A is larger for cylinders than for spheres, the predicted G_L' is larger for cylindrical dispersoids.

The volume fraction of the rigid phase, ϕ_2, is obtained directly from the total weight fraction of polystyrene in the samples. This implies that all of the polystyrene lies in domains and again overestimates the modulus of the system which undoubtedly has some polystyrene in the softer interphase.

Using Equations 1-5, the adjustable parameters of the model, ϕ_{max}, ϕ'_{max}, A and A_i are determined from the experimental G' of the sample before stretching. In the process of determining these model parameters, G_L' as well as G_U', are computed through Equations 1 and 2. The former quantity, G_L', would theoretically represent the modulus expected for a system with polystyrene dispersoids. Even though we overestimated the modulus by assuming cylindrical dispersoids, i.e., increasing A as much as reasonable, and assuming all the polystyrene lies in domains (thus maximizing ϕ_2), the predicted moduli were still low by a factor of four compared to the experimental moduli just after stretch and release for 1648, and by a factor of eight from that of 1649. In fact, for TR-41-1649 at 35°C, G_L' would equal G' (just after stretch and release) only when A, from Equation 1, was increased from 3 (determined with G' before stretching) to 48 with ϕ_{max} held constant.

Since the experimental moduli just after stretching were much greater than those predicted by G_L', we can infer - if the Nielsen model is basically correct - that the originally continuous polystyrene phase is not completely degraded to discontinuous dispersoids (not even cylinders). The fact that A must equal 48 (for TR-41-1649 at $35^{\circ}C$) before G_L' from Equation 1 (for a dispersed, rigid phase) equals the first measured G' just after stretching and releasing, suggests that the polystyrene dispersoids have such a high aspect ratio (much greater than 15) that they are no longer truly dispersed but in fact, they have either maintained or re-developed much of their original effective continuity. However, the initial reformation may be so fast that we are unable to get a datum point to represent G_L'. In other words, just after stretch and release (at t=0+) the polystyrene may be totally dispersed with no continuity among the domains but the structure quickly reforms before the first datum point can be taken. Then, subsequent structure reformation, as we observe it in these experiments, involves further conglomeration of the residual polystyrene fragments and enhancement of effective polystyrene continuity through chain diffusion to promote adhesion at the conglomerated fragment interfaces.

This idea of reformation suggests a modification of the Nielsen model by incorporating a time-dependent term in Equations 4 and 5 to account for the increasing polystyrene

continuity during reformation. In this scheme, structure

breakdown and reformation can be represented by motion along

segment AB in Figure [15] at a constant polystyrene content

ϕ_{PS}. Breakdown results in a decrease in the effective poly-

styrene continuity, ϕ_U, and movement from point A to B while

reformation results in a gradual increase in the effective

continuity, ϕ_U, and the reverse movement from B towards A.

These changes in continuity and their accompanying movement

along segment AB can be mathematically represented by incor-

porating a time-dependent reformation function R(t):

$$\phi_U = \frac{\phi_{PS}R(t) - (1-\phi'_{max})}{\phi_{max} - (1-\phi'_{max})} \quad (6) \quad \text{and} \quad \phi_L = \frac{\phi_{max} - \phi_{PS}R(t)}{\phi_{max} - (1-\phi'_{max})} \quad (7)$$

$$\text{where } 0 < R(t) \leq 1$$

At point A (Figure 15) the sample before stretching is char-

acterized by R(t) = 1.0. Just after stretching and releasing

(point B) the effective polystyrene continuity is decreased

and R(t) is much smaller than 1.0. During reformation

(point C) the effective continuity increases gradually, and

R(t) changes from its lowest value at B towards 1.0. The

quantity $\phi_{PS}R(t)$ represents the fraction of rigid material

(polystyrene) in an "equivalent" sample that would have an

identical modulus to the structure at C.

The R(t) function is fitted to each of the G' plots of

Figures 5 and 8. This is done by keeping the adjustable

parameters (ϕ_{max}, ϕ'_{max}, A, A_i) previously fitted so that the

model predicts the original (before-stretching) G'. Then

R(t) values are backed out from the observed G'(t).

These R(t) functions are used to calculate a new

function, $\phi_U(t)/\phi_U(0)$, by Eq. 6. This function

represents the fraction of the originally continuous

polystyrene that is continuous at any time, t, during re-

formation. It is a direct measure of the degree to which the

polystyrene has reformed its original effective continuity,

and hence the degree to which the structure has reformed.

Figures 16 and 17 show the calculated $\phi_U(t)/\phi_U(0)$ for

both polymers. For 1648, $\phi_U(t)/\phi_U(0)$ drops to a lower value

at 60^OC than at 35^OC, indicating that the effective polysty-

rene continuity is broken to a greater extent at 60^OC than

at 35^OC. This is consistent with the temperature effect on

structure breakdown observed with the straight-line analysis

of the G" data. At 60^OC, $\phi_U(t)/\phi_U(0)$ quickly rises above

the function at 35^OC and continues to rise for the full five

hours of the run. At 35^OC the function rises much more

slowly and appears to level out or rise imperceptibly slowly

after four hours. The differences at these two temperatures

reflect the anticipated effect of temperature on reformation,

with reformation proceeding faster at a higher temperature.

For 1649, $\phi_U(t)/\phi_U(0)$ is lower at 60^OC than at 35^OC for

the entire run, indicating that reformation is proceeding

faster at a lower temperature. This is opposite to the be-

havior of 1648 and seemingly contradicts the anticipated

temperature effect on the rate of reformation. This discrep-

ancy might initially be thought to be related to the large

difference in the interphase size between 1648 and 1649 found
by Diamant and coworkers (14-16). However, G" of 1648 and
1649 measured during reformation (Figures 6 and 9) show a
small change from the initial values which suggests
that the interphase is not strongly involved in struc-
ture recovery.   Hence, the large difference in the inter-
phase volumes between 1648 and 1649 cannot explain the tem-
perature effect on reformation in the two polymers. However,
it can be explained by invoking two different mechanisms for
structural breakdown as discussed below.

Structure Breakdown and Reformation

The mechanisms for structural breakdown involve two ex-
tremes of behavior as shown in Figure 18. The as-cast
structure is schematically represented by a lamellar mor-
phology with the polystyrene and polybutadiene segments in
their respective domains. Both are in a relaxed state with
the chains coiling randomly. Although not shown in the
figure, there is a large degree of interconnections (effec-
tive continuity) among the polystyrene domains so that the
material before stretching (at point 1 in Figure 19) is quite
rigid.

At point 2 the rigid polystyrene network begins to break
down and continues fragmenting with further elongation. At
300%, point 3, the structure is illustrated in Figure 18.

The two pictures in the middle ("stretched to 300%") represent the two extremes of structure breakdown. The one on the left represents the situation where the polystyrene segments are pulled out of their domains. This results in floating chains of the entire molecule or cilia with dangling polystyrene blocks in the polybutadiene phase. One bridge chain is also shown, but with the polybutadiene center block in a highly stressed state. The figure on the left represents the extreme of "disorderly" structure breakdown, where most of the displaced polystyrene blocks are mixed with the polybutadiene phase. By contrast, the figure on the right represents the situation where all of the polystyrene segments remain in their original domains, but the domains themselves split and fracture, resulting in a "clean" structure breakdown. Again, the polybutadiene in the bridge chains is in a highly stressed state. Voids and crazes have occurred in the structure, and they could equally well appear in the figure on the left.

Upon returning the sample to the stress-free state (point 4) the highly-stressed polybutadiene chains immediately draw the structure back towards its original, as-cast morphology. As shown in the lower two illustrations of Figure 18, the polystyrene domains have returned close to their original positions but the domains still lack mechanical integrity and there are cracks left from the void collapse. The reformation process in the stress-free state involves movement from point 4 b..ck to point 1 in Figure 19.

The two extremes of structure breakdown will result in two extremes of reformation behavior. The structure broken "disorderly" will reform slowly, since individual polystyrene segments must move back into domains. By contrast, the structure broken "neatly" will reform quickly, since only "healing" of the cracks is necessary.

It is important to note that these two extremes of structure breakdown and reformation represent limits to the actual behavior which lies somewhere in between, with both of these processes occurring to different extents. Several factors determine the degree to which each of these two mechanisms take place. Temperature would certainly be a strong factor, with more segments pulled out at higher temperatures and more domains cracked (and crazing propagation) at lower temperatures. More domains would be expected to fracture when the continuity among the polystyrene domains is low, i.e., with many "thin spots" in the connections. The presence of such weak continuity also leads to low yield stresses. Conversely, more segments would be pulled out when the continuity is high, and hence the yield stress is high. This reflects the different energy requirements for the two mechanisms. All of the factors affecting the structure breakdown mechanism are interrelated in a complex fashion through the energy requirements supplied either in the form of heat

reflected by the significantly greater yield stress of 1649 (4). At 35°C, domain cracking predominates, as with 1648, resulting in a "clean" structure breakdown. However, at 60°C the polystyrene is soft enough, and there is enough mechanical and thermal energy supplied to the material to cause displacement of individual chains from the domains, and the resulting structure breakdown is more "disorderly" than at 35°C.

The existence of two different structure breakdown mechanisms explains the observed reformation behavior in the two polymers. The weak connections in 1648 are broken "cleanly" at both temperatures so that reformation involves the highly stressed polybutadiene chains drawing the structure back towards its original morphology with gradually increasing polystyrene continuity as chains diffuse to promote adhesion at the cracks. This is an activated process so that reformation proceeds faster at 60°C than at 35°C (Figure 16). In 1649, however, two different structure breakdown processes occur at the two different temperatures. At 35°C, the polystyrene connections break apart resulting in a "clean" structure breakdown with reformation involving, as with 1648, the polybutadiene drawing the structure back together and the healing of the cracks with gradually increasing polystyrene continuity. However, at 60°C, polystyrene segments have been dragged into the interphase so that reformation is considerably more difficult. First, there are fewer stressed polybutadiene chains to "pull" the structure

(temperature effect) or mechanical energy (yield-stress effect).

Our proposed structure breakdown-reformation process is capable of explaining the difference in the temperature dependence of the $\phi_U(t)/\phi_U(O)$ curves of 1648 and 1649. Recall that an examination of reformation at a particular temperature is preceded by stretching and releasing the samples at that same temperature. The reformation in 1648 proceeds faster at 60^OC than at 35^OC. We postulate that in the preceding structure breakdown (at both temperatures) domain cracking and crazing is more important than pulling polystyrene segments out of domains. Because 1648 contains only 29% polystyrene, the interconnections within the polystyrene domains are weak, with many "thin spots", as reflected by the low yield stress (4). During the application of mechanical energy through sample elongation, the lower energy requirement to break these weak interconnections is met sooner than the higher energy requirement to pull polystyrene segments ou⁺ of domains. Even at the higher temperature, we hypothesize that the additional thermal energy is not a large enough supplement to the mechanical energy to displace individual polystyrene chains from their domains. Thus, the weak connections simply break apart before polystyrene segments are pulled out of their domains, even at the higher temperature.

However, 1649 contains much more polystyrene so that a stronger connectivity prevails among the domains, as

back together. But in addition, diffusion of polystyrene segments out of the interphase and back into domains must take place. Thus, it requires much longer to recover the original effective polystyrene continuity. This explains why reformation is slower at 60°C than at 35°C for TR-41-1649 (Figure 17).

Some evidence in the literature supports our proposed structure breakdown-reformation mechanisms. Kaelble and Cirlin (43) showed that polystyrene fragments under high deformation behave as physical crosslinks only below 40°C. They suggested that elongating the samples at higher temperatures, such as 60°C in this study, causes polystyrene segments to be pulled out of their domains and the domains cease behaving as crosslinks. Micrographs of a sample at high elongation show cavity formation in the structure. After release, micrographs reveal cracks which were attributed to the collapse of cavities. Niinomi and coworkers (39) present micrographs of stretched and released SBS-polystyrene blends that show parallel striations in the polystyrene regions which disappear upon annealing. They suggested that these may be crazes formed by the stretching process, similar to our picture of the structure after releasing from 300%. In addition, their micrographs show an increase in the amount of white areas within the structure which may be due to polystyrene blocks being dragged out of their domains. Leblanc (34) found that the hardness of block copolymers immediately after stretch and release was different from that

predicted by the intercept (t=0) of the hardness versus log
time plot. At 50°C and 60°C the material was softer than
predicted, while at 40°C the material was harder than pre-
dicted. This suggests that a different structure breakdown
process occurs at different temperatures. Below 40°C, the
structure is broken "cleanly" so that the elastomeric chains
efficiently draw the structure back closer to its original
morphology and effective polystyrene continuity. Thus, re-
formation proceeds quickly so that the material is harder
than predicted. At 50°C and 60°C the breakdown is much more
"disorderly", so that the elastomeric chains cannot draw the
structure as far back to its original morphology and effec-
tive polystyrene continuity. This lack of polystyrene con-
tinuity leaves the polybutadiene more "exposed" so that the
material is softer than predicted. Thus, analogous to our
results with 1649, reformation proceeds slower, and hence to
a lower degree of completion at the higher temperatures re-
flected by a softer material at higher temperatures.

Interphase Behavior

Our analysis so far has focused only on G', which is
correlated with the state of polystyrene phase connectivity.
The behavior of the interphase during elongation and after
release of strain has not been discussed. As noted previous-
ly the height and shape of G" in the plateau region between
the two glass transitions are strongly influenced by the

amount of material in the interphase and the composition profile across it. A mathematical model was developed (14-16) to predict the G" and G' for block copolymers with a given interphase volume fraction and composition profile. The system with a sharp interface (complete phase separation with no material in the interphase) resulted in a predicted plateau in G" nearly an order of magnitude lower than the experimental curve, while only a diffuse interphase gave the correct predictions. Yet, G' was essentially independent of the interphase. These results have an important consequence in our study.

In analyzing the G' data with the Nielsen equations we determined the volume fraction of rigid material by assuming all the polystyrene lies in a polystyrene domain, and hence a sharp interface separates it from the polybutadiene domain. In view of the aforementioned results, this simplification cre. o major error in G' calculations.

This study consistently reveals very little difference between the G" of reforming structures and the G" before stretching (Figures 6 and 9). This indicates that the interphase is largely unperturbed, which may possibly be due to very rapid reformation before the first measurements can be taken. There does appear to be a small decrease in G" following stretch and release which indicates a slight reduction of the interphase followed by a slow return to its original state.

These results provide new insights as to whether the

stress-softening effect can be attributed to interphase or polystyrene connectivity breakdown. Rather than attributing the morphological variations to one fixed mechanism, our results indicate that both interphase alteration and polystyrene connectivity breakdown processes may be involved in the observed stress-softening effect.

Comparison with Tensile Experiments

Our proposed structure after stretch and release will have a wide range of behavior depending on the scale, or amplitude, of the applied deformation monitoring structure reformation. The structure has returned close to its original morphology except for the small decrease in effective polystyrene continuity evidenced by the residual cracks in domains. But the contact surfaces of the agglomerated domains still require substantial time to "heal" by molecular diffusion of the polystyrene blocks. Hence, under second-cycle large deformation the superficial connectivity of the newly contacted fragments can not support a load and the sample displays rubber-like behavior. This explains the stress-softening observed in the second loading cycle of the stress-strain diagram. However, under small-amplitude deformation there is sufficient interaction among the polystyrene near the cracks so that the once-fragmented polystyrene still acts as it did in the original structure. Hence, the material displays nearly the same magnitude of G' and G" as

the original sample before stretch and release. Therefore,
different experimental techniques, i.e., small-amplitude
dynamic mechanical measurement and large tensile deformation,
will lead to vastly different conclusions regarding the mor-
phological state of the samples.

This conclusion also explains the results of Yang and
Meinecke (40) who determined both stress and energy loss
versus strain on a sample elongated through the plastic-to-
rubber transition. After the sample rested at room tempera-
ture for 24 hours, it did not reform its original stress-
strain properties but did reform its original energy loss
versus strain curves. This can be explained by the fact that
the stress-strain properties were determined under high
deformation so that the cracked polystyrene domains could
not support the stress, and hence the sample appeared rub-
bery even after 24 hours. The energy loss properties, how-
ever, were determined by applying a small-angle sinusoidal
strain to a sample held at a fixed elongation. At small
elongation there was sufficient interaction and superficial
connectivity so that after 24 hours the sample behaved as it
did before stretch and release. As the elongation was
further increased the once-created cracks opened up easily
and the sample behaved again in a rubber-like fashion.

ACKNOWLEDGMENT

REFERENCES

1. Shen, M., and H. Kawai, AIChEJ., <u>24</u> 1(1978).

2. Manson, J.A., and L.H. Sperling, "Polymer Blends and Composites," Plenum, New York (1976).

3. Childers, C.W. and G. Kraus, Rubber Chem. Tech., <u>40</u>, 1183 (1967).

4. Hashimoto, T., M. Fujimura, K. Saijo, H. Kawai, J. Diamant, and M. Shen in "Multiphase Polymers," S.L. Cooper and G.M. Estes, ed., p. 257, Am. Chem. Soc., Washington, D.C. (1975).

5. Molau, G.E., in "Block Polymers," S.L. Aggarwal, ed., p. 79, Plenum, New York (1970).

6. Nielsen, L.E., Rheol. Acta, <u>13</u>, 86 (1974).

7. Meier, D.J., J. Polym. Sci., <u>C26</u>, 81 (1969).

8. Meier, D.J., Polym. Preprints, <u>11</u>, 400 (1970).

9. Leary, D.F., and M.C. Williams, J. Polym. Sci., <u>B8</u>, 335 (1970); ibid., Phys. Ed., 345 (1973).

10. Leary, D.F., and M.C. Williams, J. Polym. Sci.-Phys. Ed., <u>12</u>, 265 (1974).

11. Helfand, E., Macromol., <u>8</u>, 552 (1975); J. Chem. Phys., <u>62</u>, 999 (1975).

12. Inoue, T., T. Soen, T. Hashimoto, and H. Kawai, Macro-molecules, <u>3</u>, 87 (1970).

13. Soen, T., T. Ono, K. Yamashita, and H. Kawai, Kolloid Z. u. Z.f. Polymer, <u>250</u>, 459 (1972).

14. Diamant, J., Ph.D. Thesis, Univ. California, Berkeley (1981).

15. Diamant, J., D.S. Soong and M.C. Williams in "Contemporary Topics in Polymer Science," vol. 4, W.J. Bailey and T. Tsuruta, ed., Plenum Press, N.Y. (1981) - in preparation.

16. Diamant, J., D.S. Soong and M.C. Williams in "Proceedings ANTEC Symposium on Thermoplastic Elastomers," S.P.E. (1981) - in preparation.

17. Matsuo, M., Japan Plastics, <u>2</u>(3), 6 (1968).

18. Holden, G., E.T. Bishop, and N.R. Legge, J. Polym. Sci., <u>C26</u>, 37, (1969).

19. Kerner, E.H., Proc. Phys. Soc., <u>B69</u>, 808 (1956).

20. Christensen, R.M., J. Mech. Phys. Solids., <u>17</u>, 23 (1968).

21. Dickie, R.A., J. Appl. Polym. Sci., <u>17</u>, 45 (1973).

22. Takayanagi, M., Proc. 4th Internat. Congress Rheol.,
    Part 1, Interscience, N.Y., 1965, p. 161.

23. Halpin, J.C., J. Compos. Mater., 3, 732 (1969).

24. Tsai, S.W., U.S. Dept. of Commerce, AD834851 (1968).

25. Aggarwal, S.L., R.A. Livigni, L.F. Marker, and T.J.
    Dudek, in "Block and Graft Copolymers," J.J. Burke and
    V. Weiss, ed., Syracuse Univ. Press, N.Y. (1973).

26. Beecher, J.F., L. Marker, R.D. Bradford, and S.L.
    Aggarwal, J. Polym. Sci., C26, 117 (1969).

27. Kalfoglou, N.K., J. Appl. Polym. Sci., 23, 2673 (1979).

28. Pedemonte, E., A. Turturro and G. Dondero, Br. Polym. J.,
    6, 277 (1974).

29. Akovali G., J. Diamant, and M. Shen, J. Macromol. Sci.-
    Phys., B13(1), 117 (1977).

30. Chen, Y.D.M., R.E. Cohen, J. Appl. Polym. Sci., 21,
    629 (1977).

31. Pedemonte, E., G. Dondero, G. Alfonso and F. de Candia,
    Polymer, 16, 531 (1975).

32. Keller, A., and J.A. Odell, Polym. Engin. and Sci., 17,
    544 (1977).

33. Keller, A., and M.J. Folkes, Polymer, 12, 222 (1971).

34. Leblanc, J.L., J. Appl. Polym. Sci., $\underline{21}$, 2419 (1977).

35. Dawkins, J.V., in "Block Copolymers," D.C. Allport and W.H. Janes, ed., Wiley (1973).

36. Estes, G.M., S.L. Cooper and A.V. Tobolsky, J. Macromol. Sci.-Revs. Macromol. Chem., C4(2), 313 (1970).

37. Aggarwal, S.L., Polymer, $\underline{17}$, 938 (1976).

38. Canter, N.H., J. Polym. Sci., A-2, $\underline{6}$, 155 (1968).

39. Niinomi, M., G. Akovali and M. Shen, J. Macromol. Sci.-Phys., B13(1), 133 (1977).

40. Yang, R.M. and E.A. Meinecke, Rubber Chem. Tech., $\underline{53}$, 1124 (1980).

41. Guth, E., Rubber Chem. Technol., $\underline{18}$, 596 (1945).

42. Kaelble, D.H., E.H. Cirlin, and M. Shen in "Colloidal and Morphological Behavior of Block and Graft Copolymers," G.E. Molau, ed., Plenum, New York (1971).

43. Kaelble, D.H. and E.H. Cirlin, J. Polym. Sci., Symp. No. 43, 131 (1973).

44. Halpin, J.C. and H.W. Polley, J. Comp. Mater., $\underline{1}$, 64 (1967).

45. Nielsen, L.E., ASTM Bull. No. 165, 48, April, 1950.

46. Nielsen, L.E., Rev. Sci. Instr., $\underline{22}$, 690 (1951).

Table 1.   Composition and Molecular Specifications
of the Test Samples

	TR-41-1649	TR-41-1648
	SBS (0.482 PS)	SBS (0.293 PS)
M_{S1}	14,000	16,000
M_B	30,000	78,000
M_{S2}	14,000	16,000
M	58,000	110,000

Polybutadiene Microstructure

cis 1,4	40%
trans 1,4	50%
1,2	10%

Samples cast from solution: 90/10 THF/MEK (Volume Ratio)
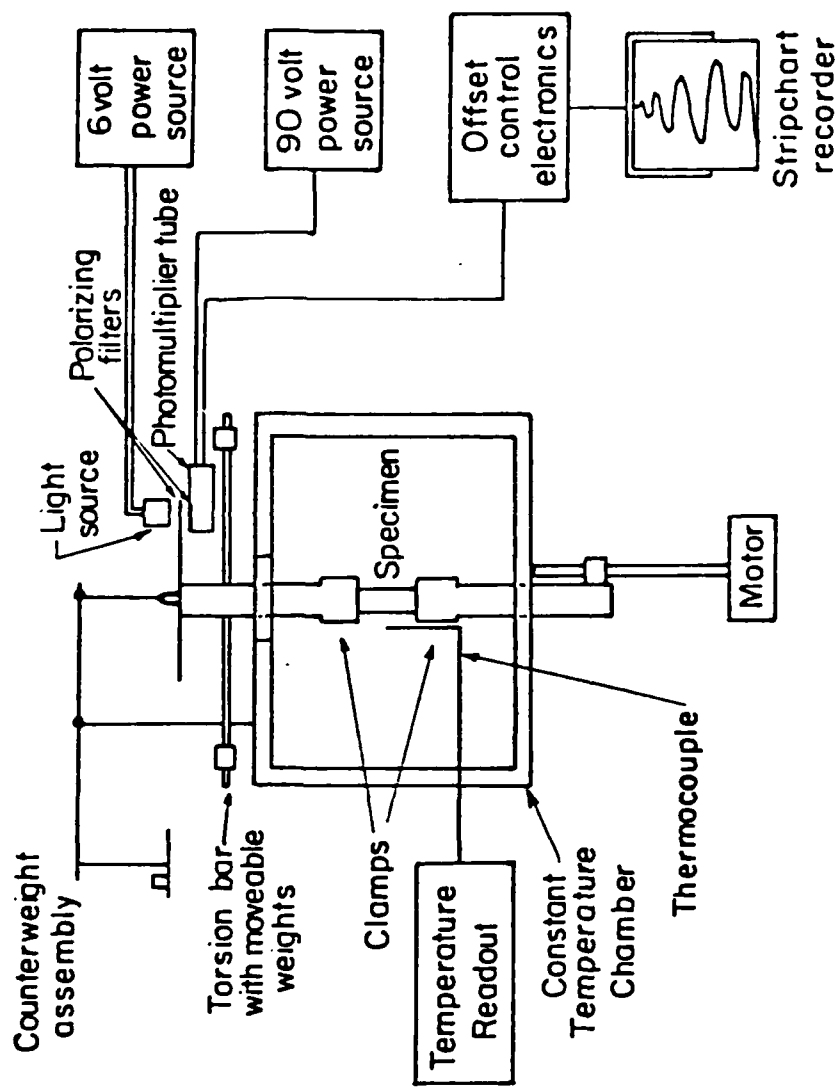
Figure 1. Modified torsion pendulum
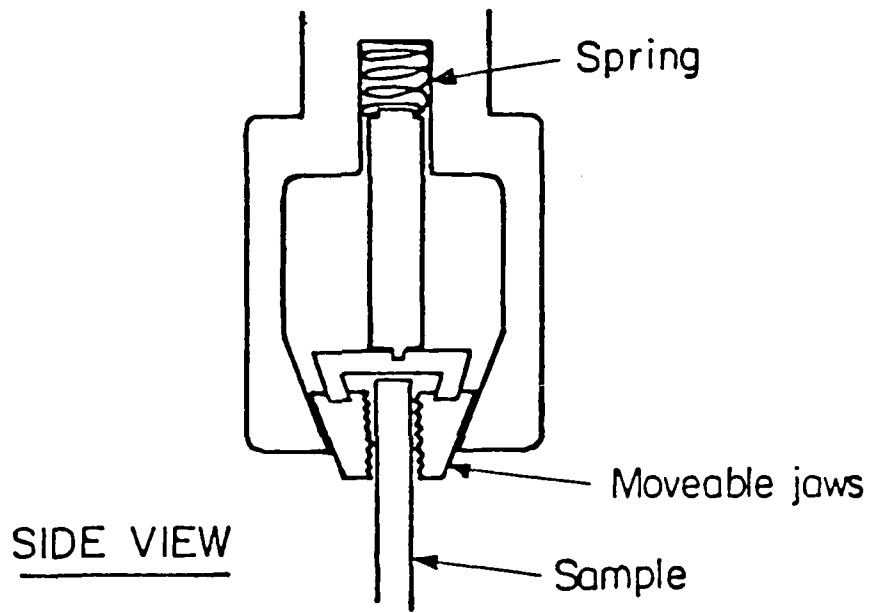
Figure 2. Sample holding system
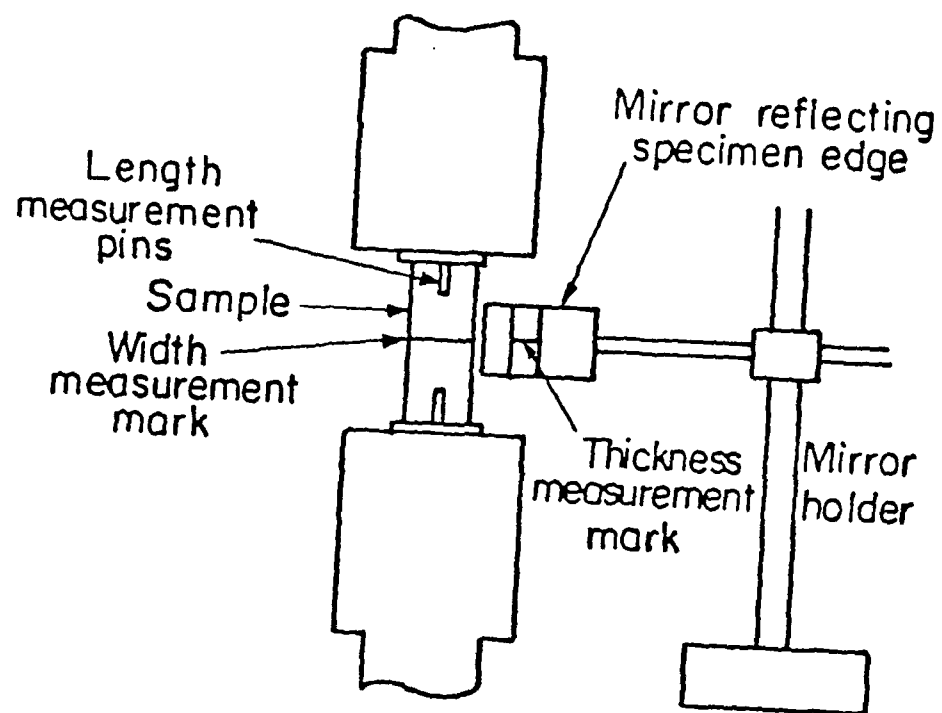
Figure 3. Experimental setup for dimension measurements
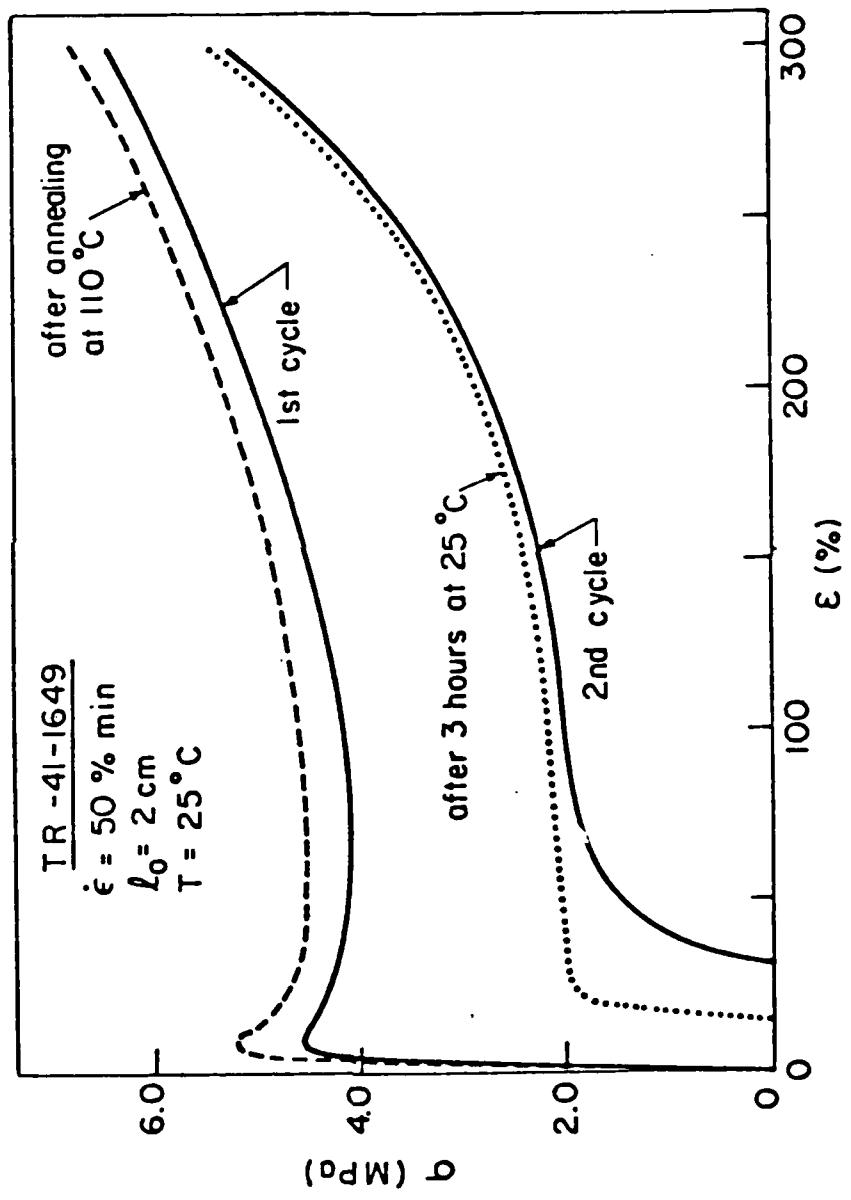
Figure 4. Stress-strain properties of TR-41-1649 following different strain and thermal histories
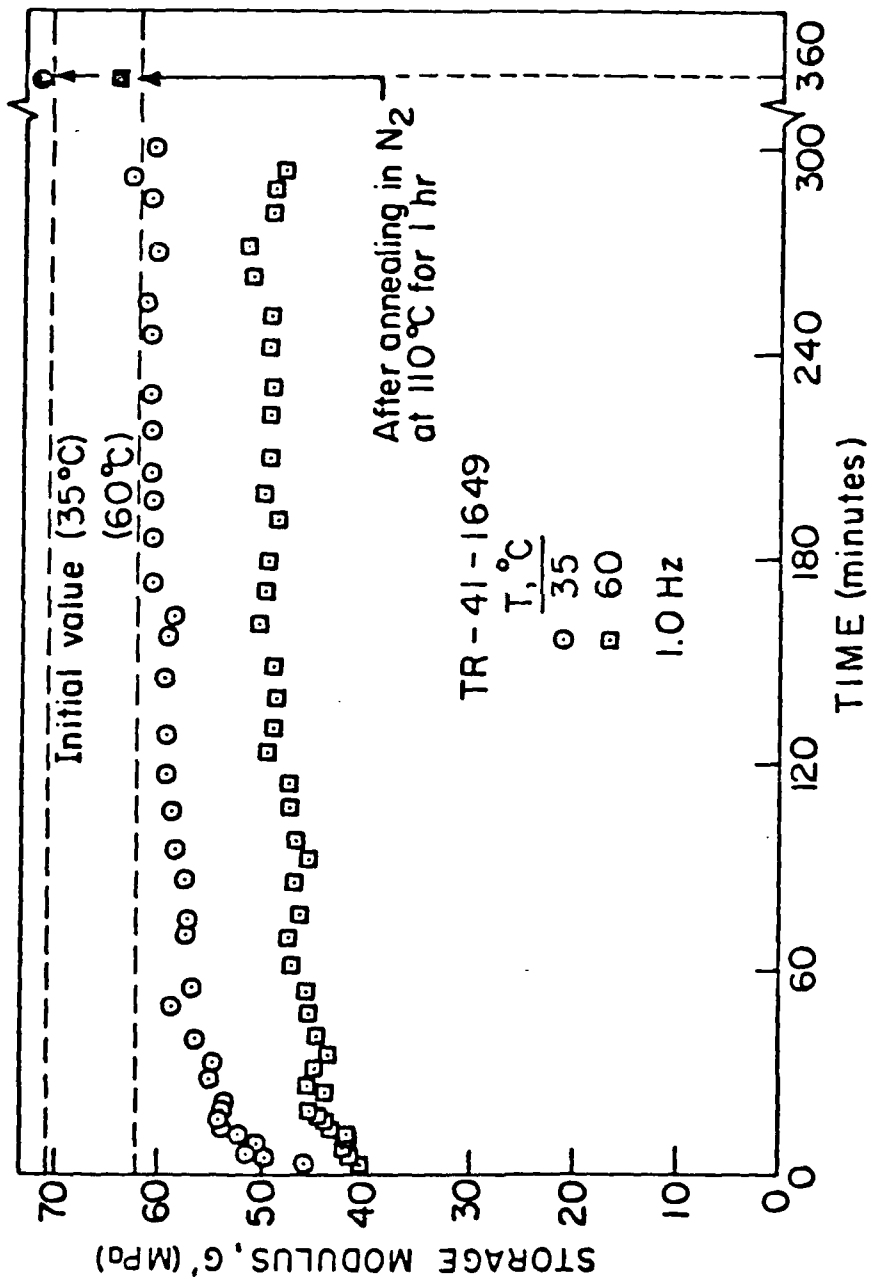
Figure 5   Storage modulus versus time after stretch and
release for TR-41-1649
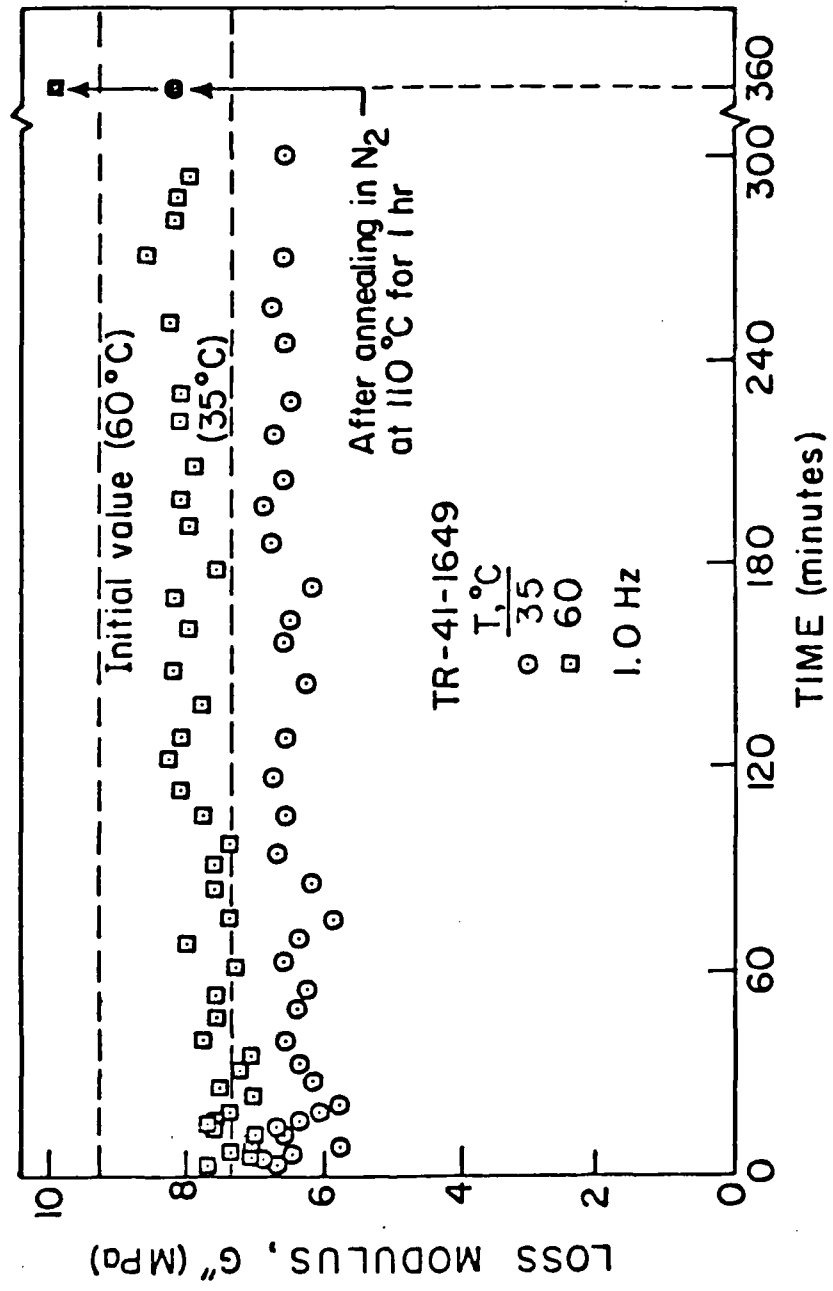
Figure 6   Loss modulus versus time after stretch and release for
TR-41-1649
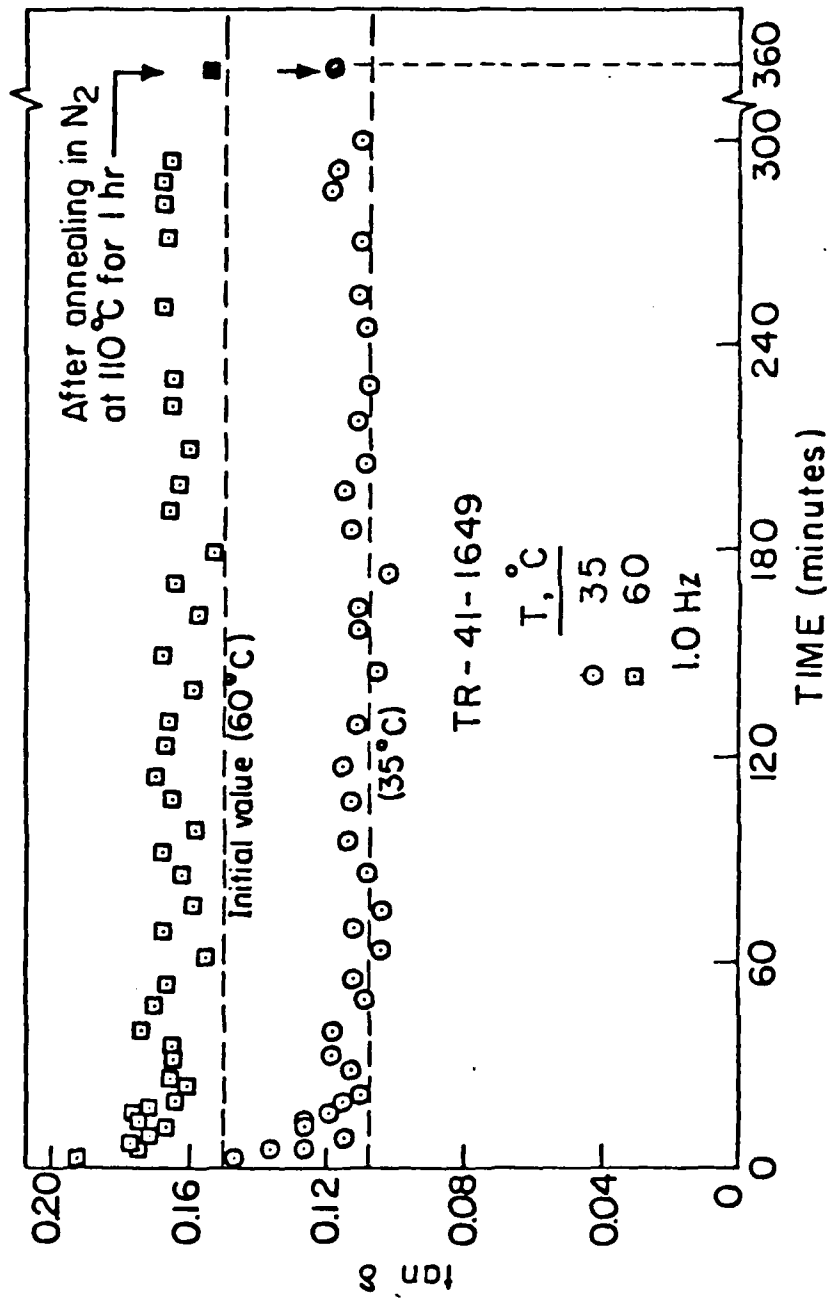
Figure 7   Tan δ versus time after stretch and release for
TR-41-1649
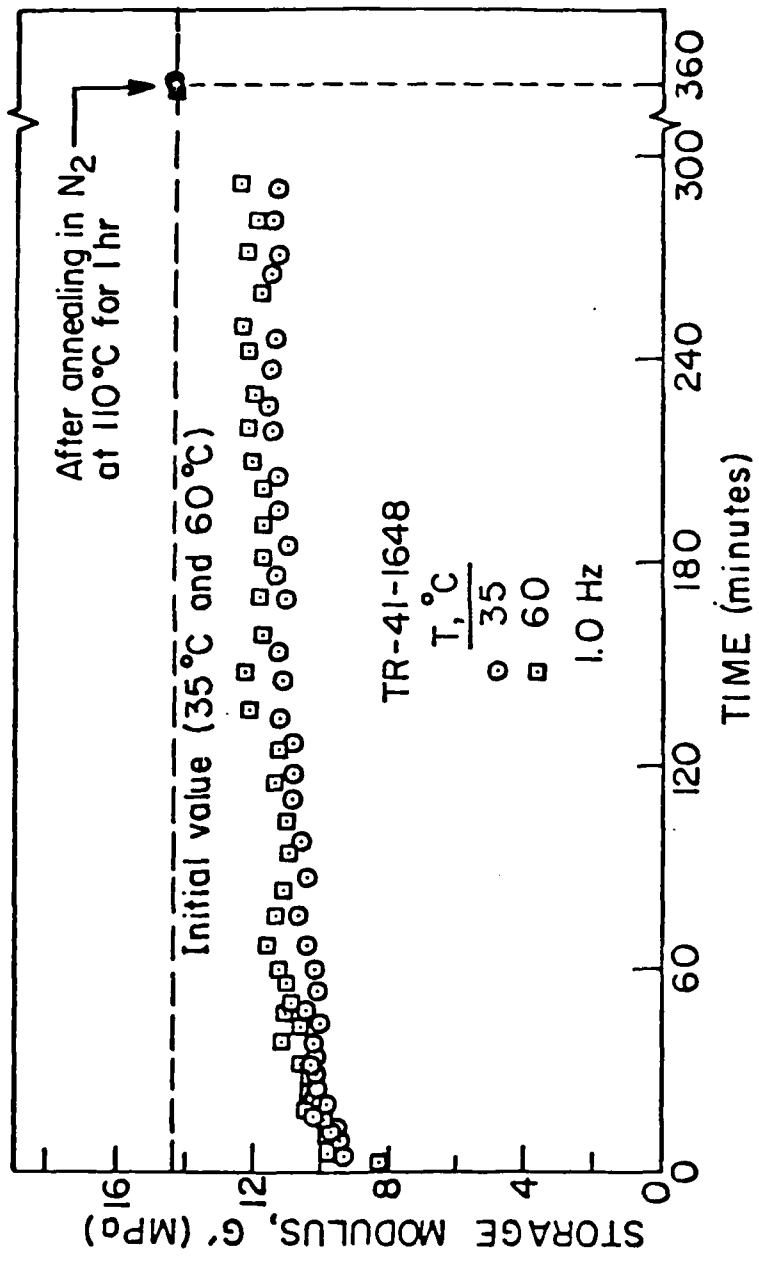
Figure 8   Storage modulus versus time after stretch and release
            for TR-41-1648
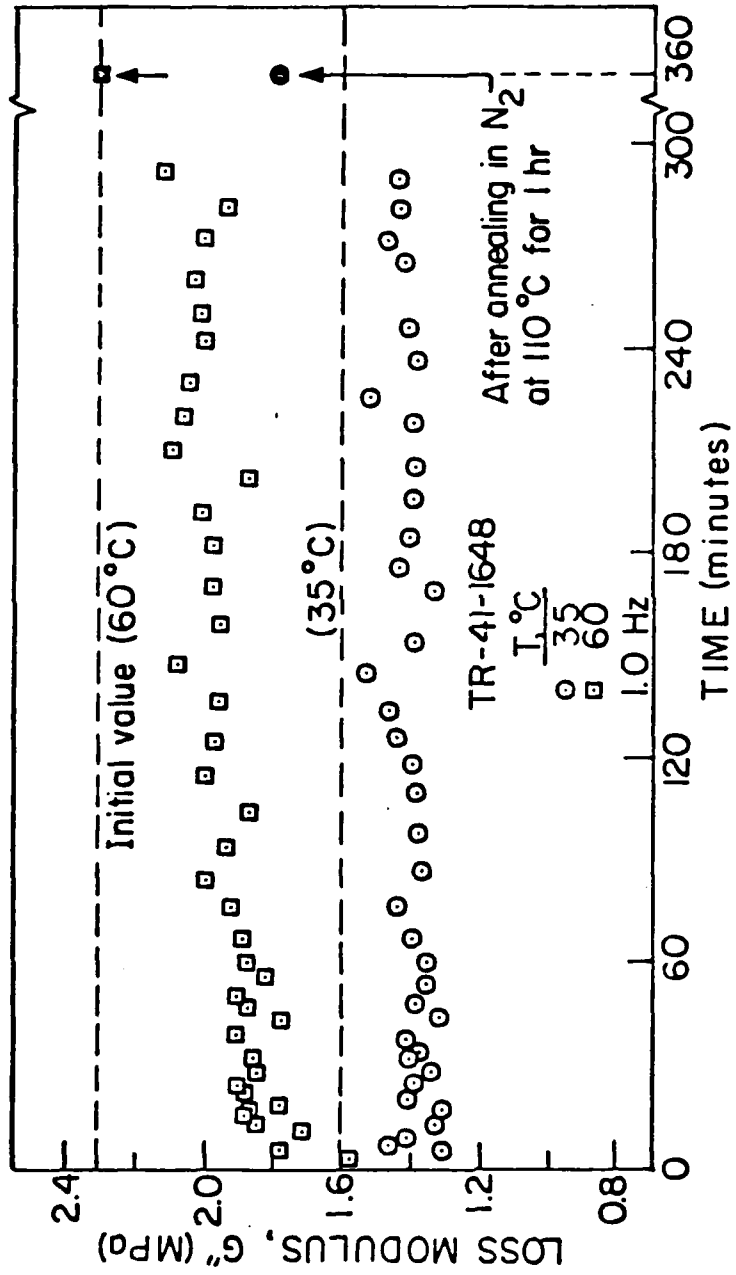
Figure 9 Loss modulus versus time after stretch and release for TR-41-1648
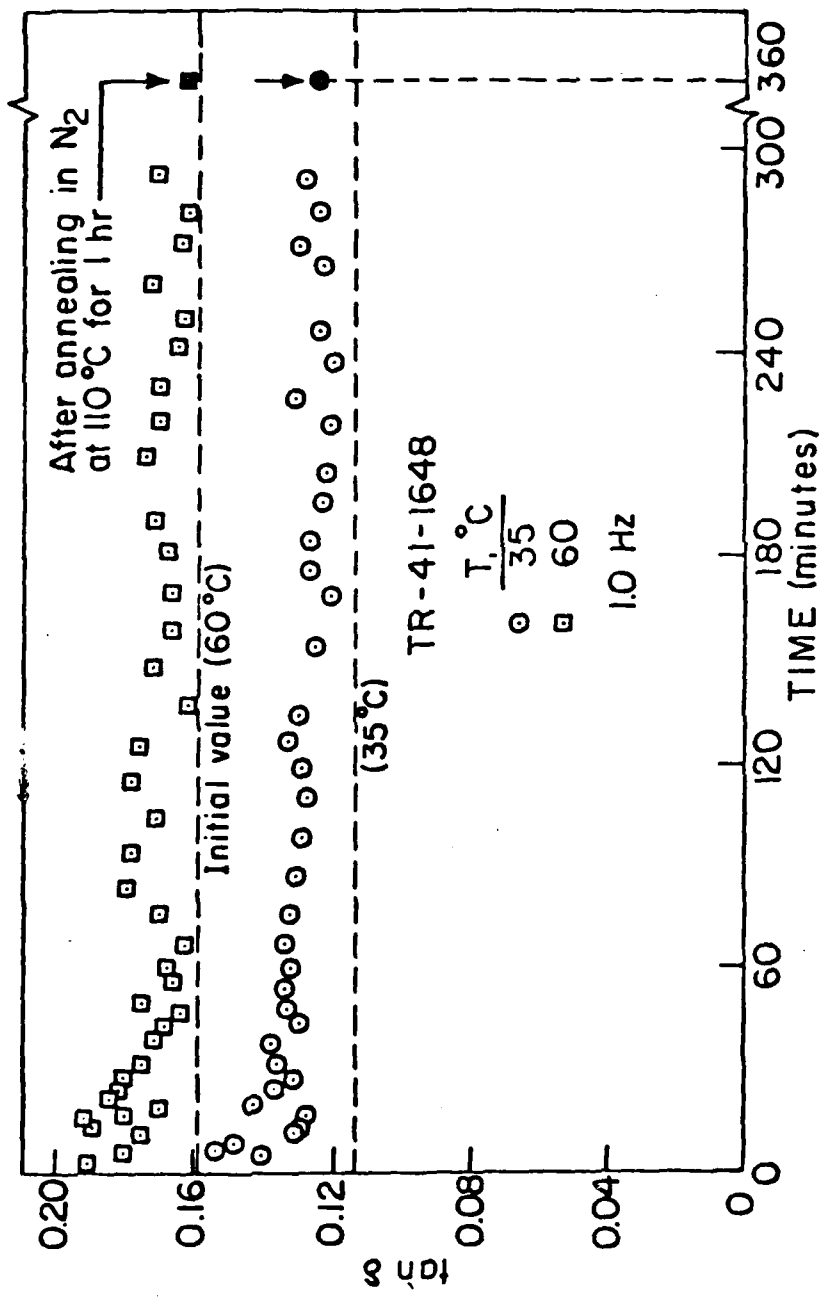
Figure 10 Tan δ versus time after stretch and release for
TR-41-1648
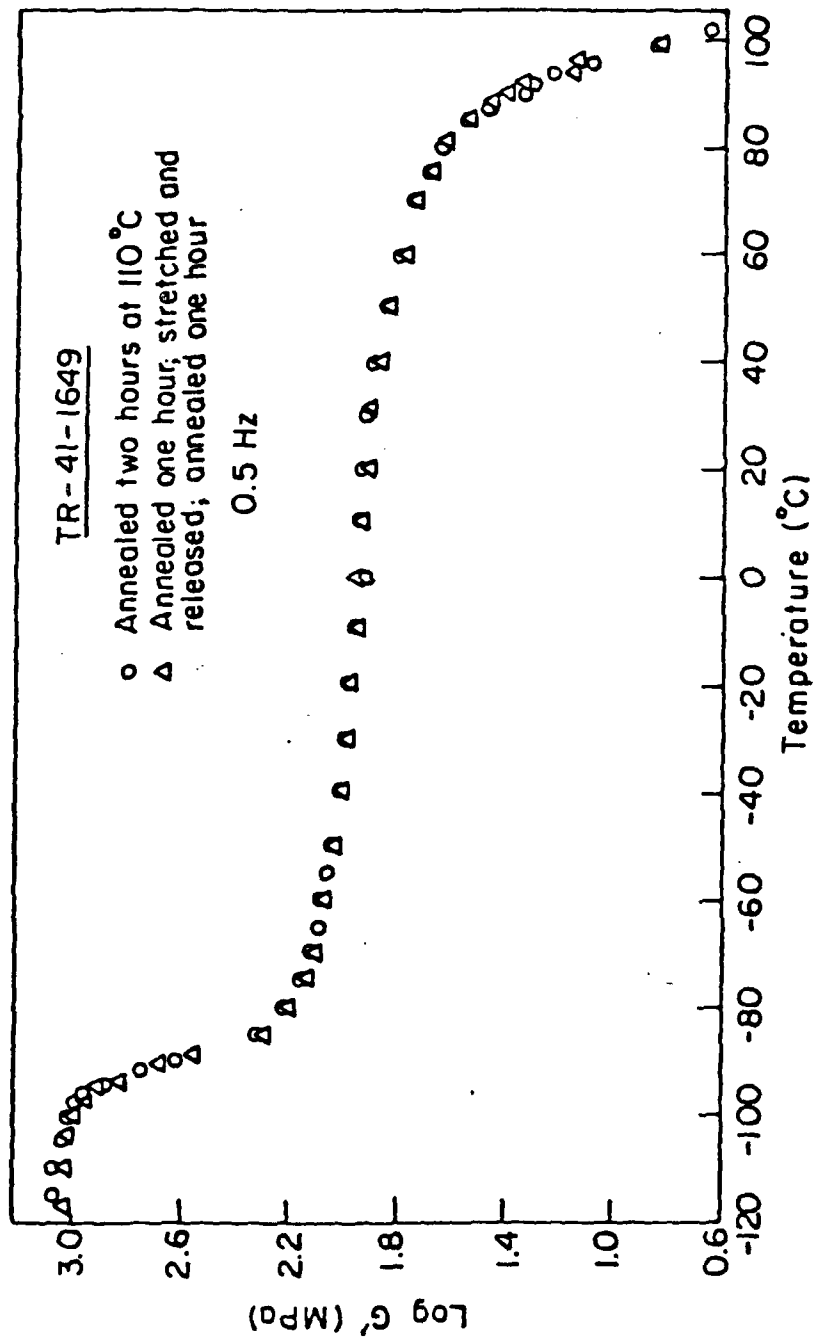
Figure 11   Log storage modulus versus temperature for TR-41-1649
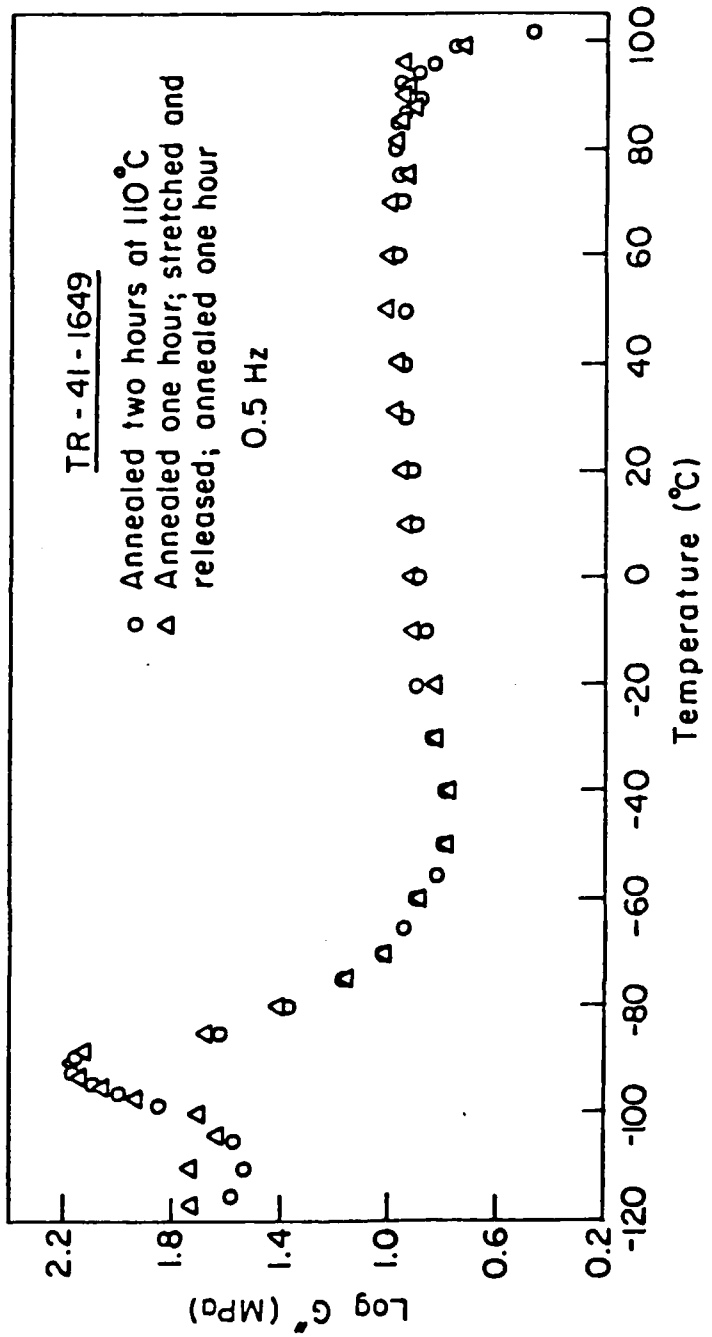
Figure 12 Log loss modulus versus temperature for TR-41-1649
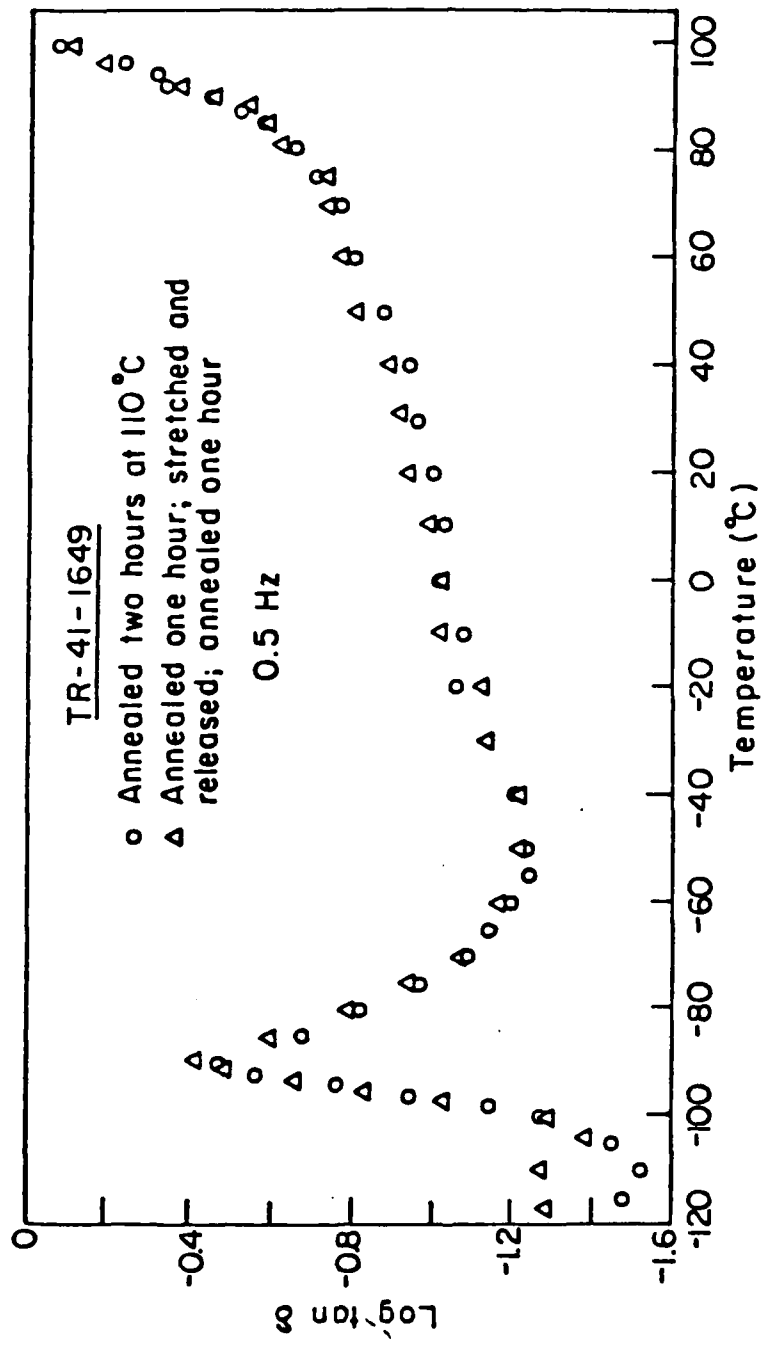
Figure 13 Log tan δ versus temperature for TR-41-1649
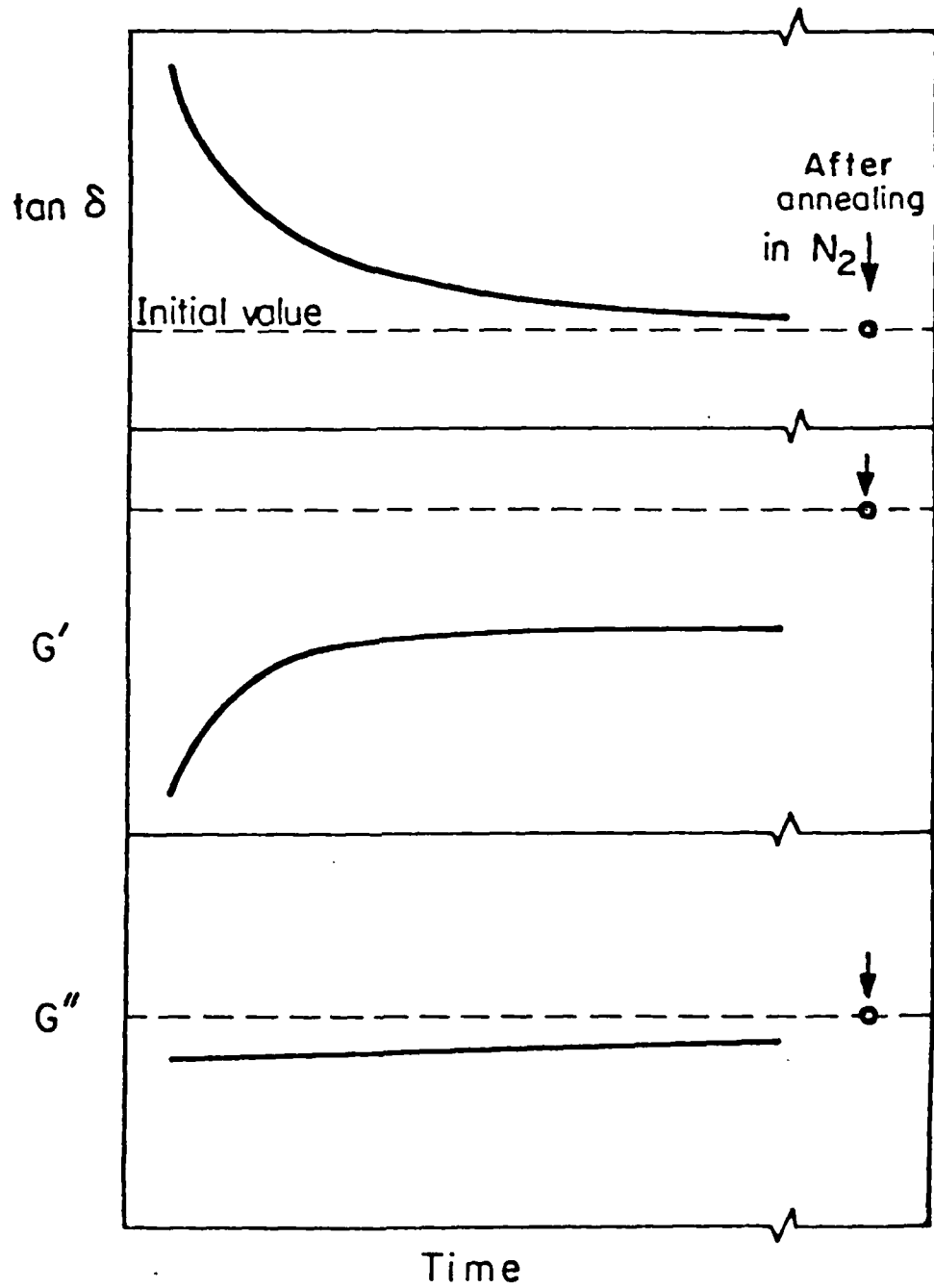
Figure 14 A schematic representation of the visco-
elastic properties of SBS block copolymers
during structure reformation
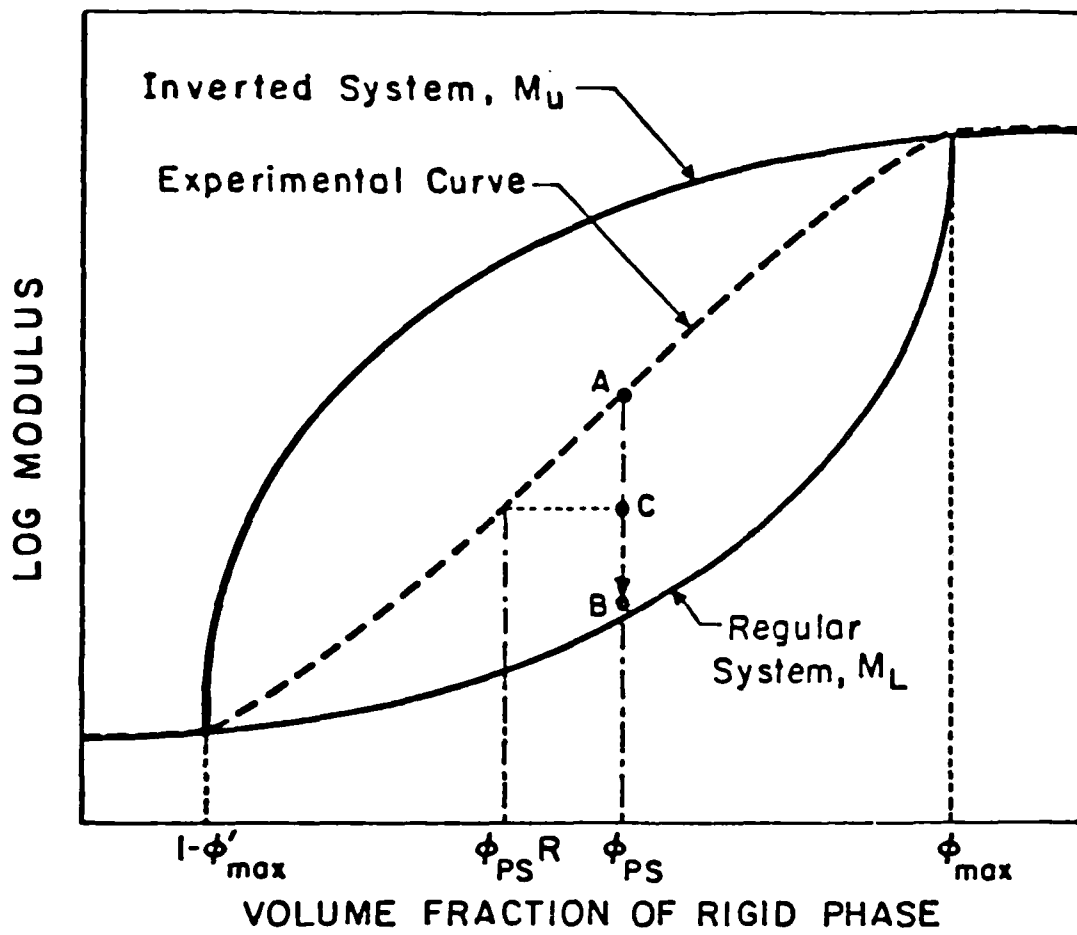
Figure 15 Predictions of the Nielsen Model and its ap-
plication to block copolymers undergoing mor-
phological variation. The maximum volume frac-
tions beyond which the major phase becomes
solely continuous are ϕ_{max} and ϕ'_{max} for the
rigid and soft phases. The upper and lower
solid curves correspond to the inverted and
regular systems, respectively. The experi-
mental modulus versus composition curve re-
flects a combination of the idealized
structures between $1-\phi'_{max}$ and ϕ_{max}. Structure
breakdown of a sample with polystyrene volume
fraction, ϕ_{PS}, is represented by motion from A
to B. At C, during structure reformation, the
modulus is equivalent to that of a sample with
polystyrene fraction, $\phi_{PS}R$
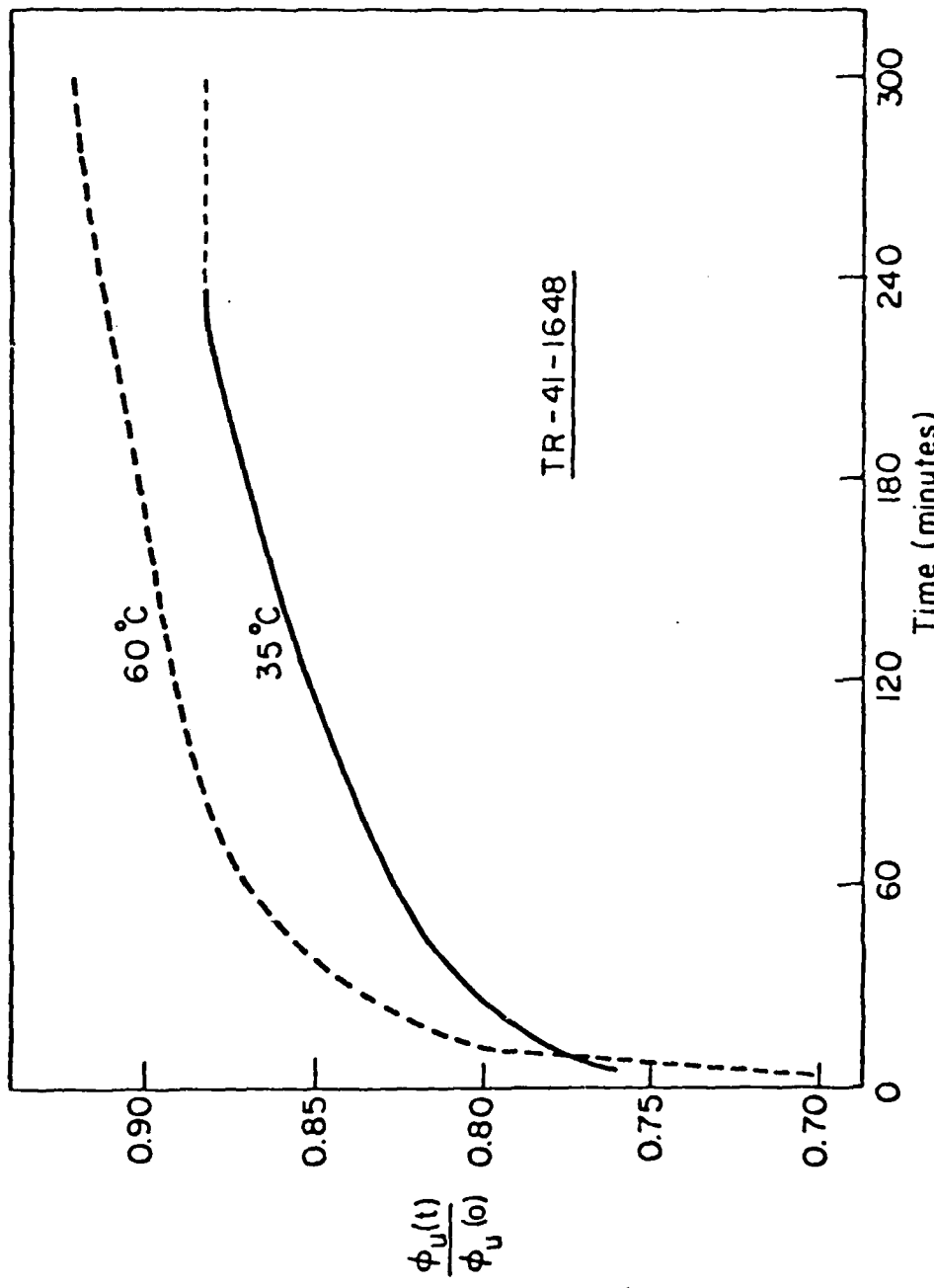
Figure 16 $\phi_U(t)/\phi_U(0)$ as a function of time after stretch and release for TR-41-1648
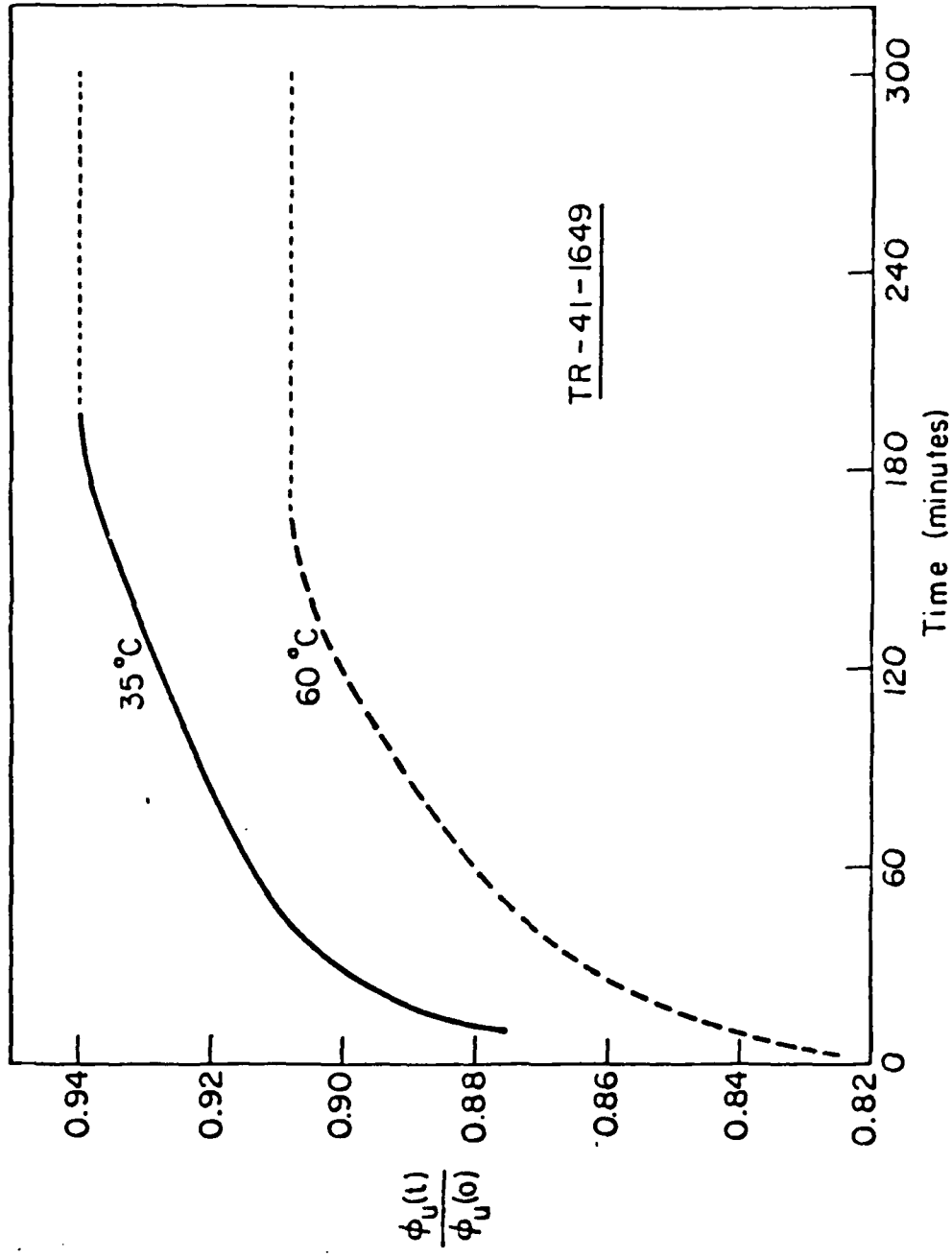
Figure 17. $\phi_U(t)/\phi_U(0)$ as a function of time after stretch and release for TR-41-1649
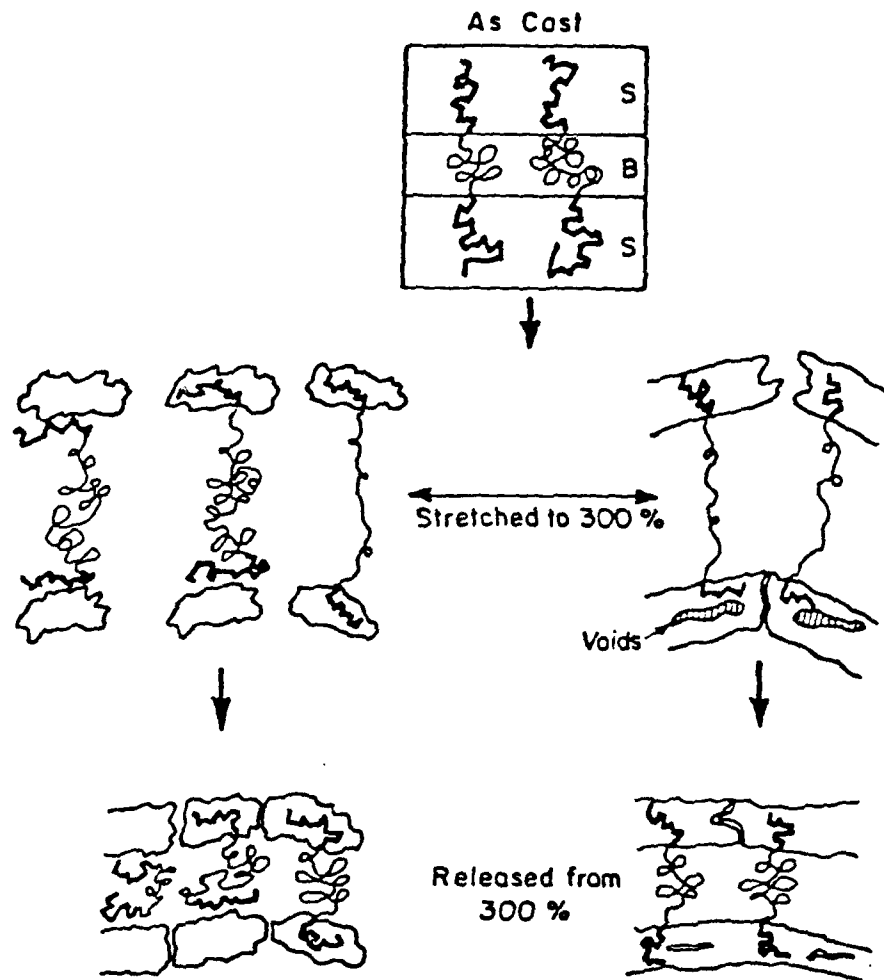
Figure 18   Proposed mechanisms of structure breakdown
and reformation. The original structure
and those prevalent when the sample is
stretched to 300% elongation and immediately
after release are illustrated by the top,
middle and bottom pictures, respectively.
Two types of breakdown behavior are pro-
posed, void formation and crazing in the
rigid phase (right figures) and block pull-
out (left figures). The actual process is
a combination of these extremes; their
relative importance depends on system
characteristics such as sample composition
and temperature
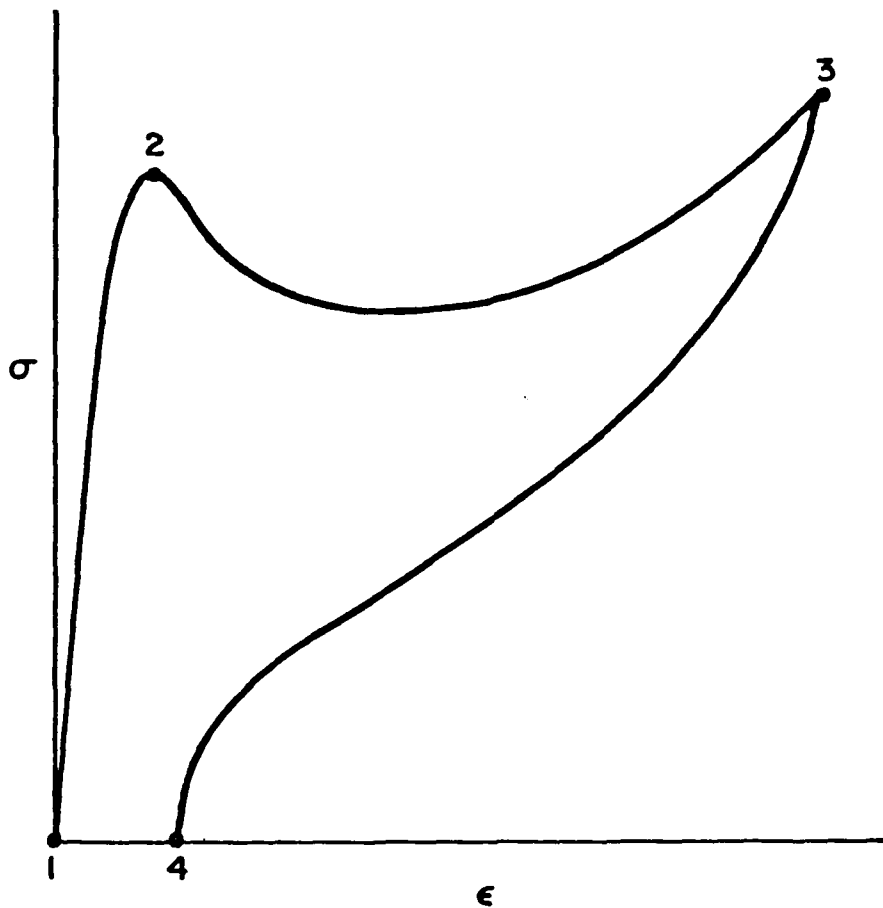
Figure 19 A schematic representation of the stress-
strain curve of a block copolymer in the
first loading (1 to 3) and unloading (3 to
4) cycle. A yield point occurs at 2, in-
dicating substantial structure degradation.
Upon annealing after the first cycle, the
sample retrieves its original length
(4 to 1)

TECHNICAL REPORT DISTRIBUTION LIST, 356A

	No. Copies		No. Copies

Dr. Stephen H. Carr
Department of Materials Science
Northwestern University
Evanston, Illinois 60201 — 1

Dr. M. Broadhurst
Bulk Properties Section
National Bureau of Standards
U.S. Department of Commerce
Washington, D.C. 20234 — 2

Professor G. Whitesides
Department of Chemistry
Massachusetts Institute of Technology
Cambridge, Massachusetts 02139

Dr. D. R. Uhlmann
Department of Metallurgy
and Material Science
Massachusetts Institute
of Technology
Cambridge, Massachusetts 02139 — 1

Naval Surface Weapons Center
Attn: Dr. J. M. Augl,
Dr. B. Hartman
White Oak
Silver Spring, Maryland 20910 — 1

Dr. G. Goodman
Globe Union Incorporated
5757 North Green Bay Avenue
Milwaukee, Wisconsin 53201 — 1

Professor Hatsuo Ishida
Department of Macromolecular Science
Case-Western Reserve University
Cleveland, Ohio 44106 — 1

Dr. David Soong
Department of Chemical Engineering
University of California
Berkeley, California 94720

Dr. Curtis W. Frank
Department of Chemical Engineering
Stanford University
Stanford, California 94305

Picatinny Arsenal
Attn: A. M. Anzalone, Building 3401
SMUPA-FR-M-D
Dover, New Jersey 07801 — 1

Dr. J. K. Gillham
Department of Chemistry
Princeton University
Princeton, New Jersey 08540 — 1

Dr. E. Baer
Department of Macromolecular
Science
Case Western Reserve University
Cleveland, Ohio 44106 — 1

Dr. K. D. Pae
Department of Mechanics and
Materials Science
Rutgers University
New Brunswick, New Jersey 08903 — 1

NASA-Lewis Research Center
Attn: Dr. T. T. Serofini, MS-49-1 — 1
21000 Brookpark Road
Cleveland, Ohio 44135

Dr. Charles H. Sherman
Code TD 121
Naval Underwater Systems Center
New London, Connecticut 06320 — 1

Dr. William Risen
Department of Chemistry
Brown University
Providence, Rhode Island 02192 — 1

Dr. Alan Gent
Department of Physics
University of Akron
Akron, Ohio 44304 — 1

Mr. Robert W. Jones
Advanced Projects Manager
Hughes Aircraft Company
Mail Station D 132
Culver City, California 90230 — 1

TECHNICAL REPORT DISTRIBUTION LIST, 356A

	No. Copies		No. Copies

Dr. C. Giori
IIT Research Institute
10 West 35 Street
Chicago, Illinois 60616   1

Dr. J. A. Manson
Materials Research Center
Lehigh University
Bethlehem, Pennsylvania 18015   1

Dr. R. S. Roe
Department of of Materials Science
  and Metallurgical Engineering
University of Cincinnati
Cincinnati, Ohio 45221   1

Dr. R. F. Helmreich
Contract RD&E
Dow Chemical Co.
Midland, Michigan 48640   1

Dr. Robert E. Cohen
Chemical Engineering Department
Massachusetts Institute of Technology
Cambridge, Massachusetts 02139   1

Dr. R. S. Porter
Department of Polymer Science
  and Engineering
University of Massachusetts
Amherst, Massachusetts 01002   1

Dr. T. P. Conlon, Jr., Code 3622
Sandia Laboratories
Sandia Corporation
Albuquerque, New Mexico   1

Professor Garth Wilkes
Department of Chemical Engineering
Virginia Polytechnic Institute and
  State University
Blacksburg, Virginia 24061   1

Dr. Martin Kaufmann, Head
Materials Research Branch, Code 4542
Naval Weapons Center
China Lake, California 93555   1

Dr. Kurt Baum
Fluorochem Inc.
680 S. Ayon Avenue
Azuza, California 91702   1

Professor S. Senturia
Department of Electrical Engineering
Massachusetts Institute of Technology
Cambridge, Massachusetts 02139   1

Professor C. S. Paik Sung
Department of Materials Sciences and
  Engineering Room 8-109
Massachusetts Institute of Technology
Cambridge, Massachusetts 02139   1

Dr. T. J. Reinhart, Jr., Chief
Composite and Fibrous Materials Branch
Nonmetallic Materials Division
Department of the Air Force
Air Force Materials Laboratory (AFSC)
Wright-Patterson AFB, Ohio 45433   1

Professor Brian Newman
Department of Mechanics and
  Materials Science
Rutgers, The State University
Piscataway, New Jersey 08854   1

Dr. J. Lando
Department of Macromolecular Science
Case Western Reserve University
Cleveland, Ohio 44106   1

Dr. John Lundberg
School of Textile Engineering
Georgia Institute of Technology
Atlanta, Georgia 30332   1

Dr. J. White
Chemical and Metallurgical Engineering
University of Tennessee
Knoxville, Tennessee 37916   1

TECHNICAL REPORT DISTRIBUTION LIST, GEN

	No. Copies		No. Copies
Office of Naval Research Attn: Code 472 800 North Quincy Street Arlington, Virginia 22217	2	U.S. Army Research Office Attn: CRD-AA-IP P.O. Box 1211 Research Triangle Park, N.C. 27709	1
ONR Western Regional Office Attn: Dr. R. J. Marcus 1030 East Green Street Pasadena, California 91106	1	Naval Ocean Systems Center Attn: Mr. Joe McCartney San Diego, California 92152	1
ONR Eastern Regional Office Attn: Dr. L. H. Peebles Building 114, Section D 666 Summer Street Boston, Massachusetts 02210	1	Naval Weapons Center Attn: Dr. A. B. Amster, Chemistry Division China Lake, California 93555	1
Director, Naval Research Laboratory Attn: Code 6100 Washington, D.C. 20390	1	Naval Civil Engineering Laboratory Attn: Dr. R. W. Drisko Port Hueneme, California 93401	1
The Assistant Secretary of the Navy (RE&S) Department of the Navy Room 4E736, Pentagon Washington, D.C. 20350	1	Department of Physics & Chemistry Naval Postgraduate School Monterey, California 93940	1
Commander, Naval Air Systems Command Attn: Code 310C (H. Rosenwasser) Department of the Navy Washington, D.C. 20360	1	Scientific Advisor Commandant of the Marine Corps (Code RD-1) Washington, D.C. 20380	1
Defense Technical Information Center Building 5, Cameron Station Alexandria, Virginia 22314	12	Naval Ship Research and Development Center Attn: Dr. G. Bosmajian, Applied Chemistry Division Annapolis, Maryland 21401	1
Dr. Fred Saalfeld Chemistry Division, Code 6100 Naval Research Laboratory Washington, D.C. 20375	1	Naval Ocean Systems Center Attn: Dr. S. Yamamoto, Marine Sciences Division San Diego, California 91232	1
		Mr. John Boyle Materials Branch Naval Ship Engineering Center Philadelphia, Pennsylvania 19112	1

TECHNICAL REPORT DISTRIBUTION LIST, GEN

No.
Copies

Mr. James Kelley
DTNSRDC Code 2803
Annapolis, Maryland 21402   1

Mr. A. M. Anzalone
Administrative Librarian
PLASTEC/ARRADCOM
Bldg 3401
Dover, New Jersey 07801   1

DATE FILMED

8